THESIS APPROVAL

GRADUATE SCHOOL, KASETSART UNIVERSITY

Master of Engineering (Advanced and Sustainable Environmental Engineering)

DEGREE

Advanced and Sustainable Environmental Engineering — Engineering

FIELD — **FACULTY**

TITLE: Synthesis of Methanol from CO_2 Hydrogenation over CuO/ZnO/MWCNTs Catalysts

NAME: Miss Pussorn Akkarapreechakul

THIS THESIS HAS BEEN ACCEPTED BY

(Assistant Professor Thongthai Witoon, D.Eng.) **THESIS ADVISOR**

(Mr. Kajornsak Fuangnawakij,D.Eng.) **THESIS CO-ADVISOR**

(Associate Professor Thongchai Rohitatisha Srinophakun, Ph.D.) **GRADUATE COMMITTEE CHAIRMAN**

APPROVED BY THE GRADUATESCHOOL ON _____

(Associate Professor Gunjana Theeragool, D.Agr.) **DEAN**

THESIS

SYNTHESIS OF METHANOL FROM CO_2 HYDROGENATION OVER CuO/ZnO/MWCNTs CATALYSTS

PUSSORN AKKARAPREECHAKUL

A Thesis Submitted in Partial Fulfillment of
the Requirements for the Degree of
Master of Engineering (Advanced and Sustainable Environmental Engineering)
Graduate School, Kasetsart University
2015

Pussorn Akkarapreechakul 2015: Synthesis of Methanol from CO_2 Hydrogenation over CuO/ZnO/MWCNTs Catalysts. Master of Engineering (Advanced and Sustainable Environmental Engineering), Major Field: Advanced and Sustainable Environmental Engineering, Faculty of Engineering. Thesis Advisor: Assistant Professor Thongthai Witoon, D.Eng. 57 pages.

In this study, multi-wall carbon nanotubes (MWCNTs) was used to improve the catalytic performance of CuO/ZnO catalyst for methanol synthesis from CO_2 hydrogenation. The surface of MWCNTs was treated with different types of acid. The CuO to ZnO ratio was fixed at 1 and the MWCNTs content was varied from 0 to 80 wt%. The CuO/ZnO/MWCNTs catalysts were prepared by co-precipitation method and were characterized by means of N_2-sorption, Raman spectroscopy, FT-IR, XRD, SEM, TEM, TPR and N_2O pulse chemisorption. The dispersion of CuO and ZnO particles was found to be improved by acid treatment of MWCNTs. The CuO/ZnO/ MWCNTs catalysts with 60 wt% MWCNTs gave the highest yield of methanol of 104 $g_{methanol}/(kg_{catalyst}h)$.

_____ _____ __ / __ / __

Student's signature Thesis Advisor's signature

ACKNOWLEDGEMENTS

I would like to express the deepest appreciation to my thesis advisor and co-advisor Asst. Prof. Dr. Thongthai Witoon, Dr. Kajornsak Fuangnawakij and Emeritus Prof. Dr. Wiwut Tanthapanichakoon whose guidance, continuing support and assistance, which encouraged to complete this research.

I would like to thank the Advance and Sustainable environmental Engineering Program of TAIST Tokyo Tech (Thailand Advanced Institute of Science and Technology) at the faculty of Engineering, Kasetsart University, The department of Chemical Engineering, Kasetsart University and The National Nanotechnology Center (NANOTEC) under the National Science and Technology Development Agency which provide scholarship, tool and equipment for my research.

I would also like to thank all the staff and friends who always support me everything during this study.

Finally, I am largely indebted to my family for their perseverance support, patience, and understanding.

Pussorn Akkarapreechakul

October 2014

TABLE OF CONTENTS

Page

LIST OF TABLES

LIST OF FIGURES

LIST OF FIGURES (Continued)

SYNTHESIS OF METHANOL FROM CO_2 HYDROGENATION OVER CuO/ZnO/MWCNTs CATALYSTS

INTRODUCTION

Global warming has become a major catastrophic problem of the world. This has been confirmed by yearly increasing of the earth's temperature which has been effected by emission of the greenhouse gases (GHGs). The GHGs comprise water vapor (H_2O), carbon dioxide (CO_2), methane (CH_4), nitrous oxide (N_2O), ozone (O_3), and CFCs. Carbon dioxide is the most significant GHGs that released into the atmosphere by human activities (Canadell *et al.*, 2007) such as combustion of coal or hydrocarbons and fermentation of sugar in beverage industry. Carbon dioxide concentration in the atmosphere is dramatically increasing along with world population, city expansion, and huge consumption of fossil fuel. Molecules of carbon dioxide can absorb energy from infrared rays, re-emits it onto the earth surface, and increase the average global temperature. This, finally, causes climatic changes, glacial melting, and sea-level rising.

The other relating problem is oil crisis. The world's fossil fuel consumption is continuously increasing. The coal, oil, and natural gas are consumed as energy sources for production of many types of products and services (Shin, 1982). On the other hand, global supply of this fossil fuel is limited. The yearly oil production decreases by 2-5 percent every year (Friedrichs, 2010). This makes price increase rapidly (Bhar and Malliaris, 2011). Therefore, other alternative and renewable energy sources become important issues that everyone should concern.

Presently, many researches focus on processes which can convert carbon dioxide into the alternative energy such as methanol (Collins *et al.,* 2012). This is one of the best way to reduce the GHGs emission. Production of methanol from carbon dioxide is a popular method because methanol can be used as fuel and chemical feedstock in various applications such as biodiesel production, fuel cell, hydrogen carrier, electric generation, and solvents. Cu/Zn catalysts are generally used for CO_2

hydrogenation to produce methanol (Shina *et al.*, 2013; Kim *et al.*, 2013; Ko *et al.*, 2014; Rafferty *et al.*, 2011). Conversion of carbon dioxide to methanol is not practical because of its remarkabe stable (Alpers, 1990). That reaction cannot occur without a proper catalyst. The catalyst used in this reaction is that of the copper based catalyst (Ereña *et al.*, 2005).

In this study, the carbon dioxide is converted to be methanol by the carbon dioxide hydrogenation reaction using a catalyst. The catalyst is copper (Cu) and zinc (Zn) loaded on carbon nanotube (CNTs) that is functionalized with an acid solution. The study referred to this catalyst to Cu-Zn-CNT and put into a fixed bed reactor. Variation of temperature, Cu loading percent, and type of acid treated solution were studied. The catalyst was characterized by N_2-sorption, X-ray Diffraction (XRD), Scanning Electron Microscopy (SEM), Transmission Electron Microscopy (TEM), Raman Spectroscopy, Temperature Programmed Reduction (TPR), and nitrous oxide chemisorption in order to determine the best condition to produce methanol by carbon dioxide.

OBJECTIVES

1. To synthesize CuO/ZnO/MWCNTs catalyst for methanol production

2. To study effects of varying weight percentage ratio of CuO/ZnO/MWCNTs

3. To study effects of varying type of acid for carbon nanotubes treatment step

4. To study effects of varying reaction temperature

Scopes of Work

1. The ratio of CuO to ZnO was fixed at 1 and the MWCNTs was varied from 0 to 80 wt%

2. The different types of acid for treatment step include H_2SO_4, H_3PO_4 and HNO_3

3. Investigate the effects of varying reaction temperature: 220 ^oC, 250 ^oC, and 280 ^oC

LITERATURE REVIEW

Rising in carbon dioxide (CO_2) concentration in the world has been definitely caused by human activities and has become a major reason for global warming. The average global temperature is increasing rapidly (Canadell *et al.*, 2007). Many researchers have tried to study on converting of this CO_2 to be the other usefully high-commercial substrate such as hydrocarbon. Among others, methanol is the major target which can be used as fuel and chemical raw material for many applications, such as: fuel cell, hydrogen carrier, biodiesel production, electric generation, and solvent. Therefore, synthesis of methanol from CO_2 is aimed to be one essential approach to reduce impacts of the Green House Gases (GHGs). This reaction is simple called CO_2 hydrogenation. However, because the CO_2 is very stable, the specific catalyst has to be used to convert CO_2 and H_2 to be methanol (CH_3OH). The Cu-based catalyst loaded on carbon nanotube support has been selected by the present study.

1. Methanol synthesis via CO_2 hydrogenation

Hydrogenation reaction is one of the well-known reduction reaction of which the organic compound is added by hydrogen. The hydrogenated organic compound becomes more saturated. This reaction reduces double bond and triple bond in unsaturated compound. The hydrogenation reaction via homogeneous catalyst is used to prevent redissolution of polymer to an organic compound (Aungsutorn, 2009). Since the hydrogen bond in hydrogen (H-H) is a very strong bond, the hydrogenation reaction can be occurred at only high temperature in order to break the hydrogen bond and to reactivate hydrogen atoms. However, the operation under suitable catalyst would lower the reaction temperature.

Synthesis of methanol by CO_2 hydrogenation involves two reactions, methanol synthesis reaction and reverse water-gas shift reaction. The methanol synthesis reaction that is shown in equation (1) converts CO_2 and H_2 into methanol

(CH_3OH) and water (H_2O). The equation (2) is a side reaction that converts CO_2 and H_2 into carbon monoxide (CO) and water (H_2O) (Zahedic *et al*., 2007).

$$CO_2 + 3H_2 \rightleftharpoons CH_3OH + H_2O \qquad \triangle H^o = -49.5 \text{ kJ/mol} \qquad (1)$$

$$CO_2 + H_2 \rightleftharpoons CO + H_2O \qquad \triangle H^o = 41.2 \text{ kJ/mol} \qquad (2)$$

Following the equation (1), methanol synthesis step is occurred on metallic catalyst such as Cu-based catalyst. It is believed that Cu can absorb hydrogen (H_2) and the reaction takes place on Cu surface (An *et al.,* 2008). The methanol synthesis is an exothermic reaction of which total moles decrease. Regarding the thermodynamic theory, incrementation of temperature and pressure affects CO_2 conversion and increases methanol yield. However, over temperature may generate a water-gas-shift step which is an endothermic reaction and can result the decreasing of methanol production (Xin *et al.*, 2009).

There are five possible ways in the methanol production from CO_2.

The first pathway is a conventional form where HCOO, H_2COO (dioxomethylene), H_2CO, H_3CO, and methanol (CH_3OH) are respectively converted from CO_2 as shown in Figure 1.

Figure 1 1st Pathway of methanol production from carbon dioxide.

Source: Liu *et al.*(2013)

The second pathway is a modified form where CO_2 is converted to HCOO, similar to the first pathway. Subsequently, it is converted to be HCOOH (formic acid) and H_2COOH before converting to H_2CO, H_3CO and CH_3OH again (Figure 2).

In this pathway, the formic acid (HCOOH) can be formed in the number over the H_2COO.

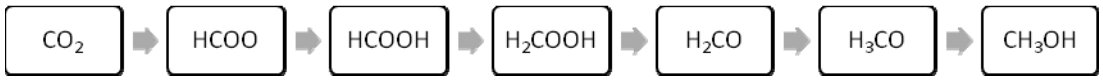

Figure 2 2nd Pathway of methanol production from carbon dioxide.

Source: Liu *et al.* (2013)

Figure 3 shows the third pathway. Moreover the hydrogenation, the carbon dioxide decomposes to form carbon monoxide and then HCO, H_2CO, H_3CO, and methanol.

Figure 3 3rd Pathway of methanol production from carbon dioxide.

Source: Liu *et al.* (2013)

Figure 4 shows the forth pathway, which is slightly different from the third pathway. The water-gas-shift reaction is occurred from HOCO intermediate.

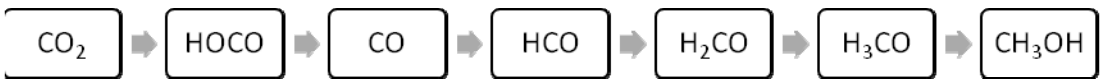

Figure 4 4th Pathway to produced methanol from carbon dioxide.

Source: Liu *et al.* (2013)

The last pathway, following the H_2O-mediated mechanism, HOCO, COHOH, COH, HCOH, H_2COH, and CH_3OH are occurred, respectively.

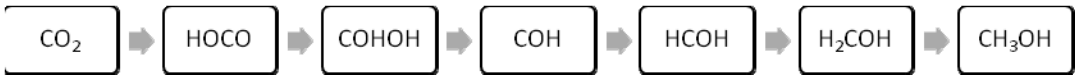

Figure 5 5th Pathway of methanol production from carbon dioxide.

Source: Liu *et al.* (2013)

The last reaction; water-gas-shift, is a side reaction. This reaction will occur when reaction temperature is high enough and it is an endothermic reaction as shown in equation 2. Figure 4, the HOCO is intermediate and its H atom will form the reverse water-gas-shift products; CO and H_2O (Liu *et al.,* 2013).

Since CO_2 is a very stable compound, the metal catalyst (Cu, Zn, Ni, Pd, Pt, Au etc.) are used in the hydrogenation reaction in order to produce methanol from CO_2 and H_2.

2. Cu/Zn based catalyst for methanol synthesis

The catalyst that used in methanol synthesis is a metal catalyst. Metal catalysts such as Pd, Ni, Pt, Ru, Rh, Cu, and Zn have been used in methanol synthesis but the most popular one are Cu and Zn. The cost of Cu and Zn is much lower than the others; therefore, they are quite active on CO_2 hydrogenation (Collins *et al.,* 2012; Bahrens *et al.,* 2012).

Normally, a suitable supporter is used together with the selected metal catalyst. The metal catalyst has to be loaded on the supporter to improve its chemical and physical properties and to increase conversion rate of substances. ZnO has been used as a supporter of the catalysts in methanol synthesis (Fujitani and Nakamura, 1998). It could improve dispersion and particle size of Cu. Moreover, their improved properties

affect the increasing of specific activity of methanol synthesis. However, ZnO using as a supporter could cause Cu particles sintering (Toyir *et al.,*2009) which, subsequently, resulted in a long time activity decreasing.

With reference to previous researches in methanol synthesis via CO_2 hydrogenation, many kinds of metal catalysts and supporters were studied and the Cu/Zn-base catalyst was found to be the most effective one. Guo *et al.* (2007)andBaltes *et al.* (2008)studied about methanol synthesis by using $CuO/ZnO/Al_2O_3$. Sun *et al.,* (1997), Jun *et al.* (1998), and Dong *et al.* (2003) focused on synthesizing of $Cu/ZnO/Al_2O_3$ catalyst for methanol synthesis. The Al_2O_3 was used as a promoter for Cu/Zn based catalyst because the using of Al_2O_3 together with ZnO can reduce the sintering of Cu particles in long time operation (Toyir *et al.,* 2009).

Sun *et al.* (1997) studied on preparation of Cu/ZnO and $Cu/ZnO/Al_2O_3$ ultrafine catalyst for methanol synthesis via CO_2 hydrogenation. The catalysts were prepared by an oxalate gel co-precipitation method and the activities were measured under 180-300 ºC and 2 MPa. Performances of methanol synthesis from CO_2 hydrogenation over various catalysts are shown in Figure 6 and Table 1. The best composition of Cu/ZnO and $Cu/ZnO/Al_2O_3$ were 50/50 and 45/45/10.

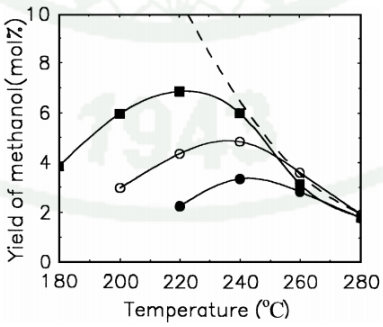

Figure 6 The catalysts activity of methanol synthesis in various temperature.
(●) Cu/ZnO (30:70), (○) Cu/ZnO (50:50) and (□) $Cu/ZnO/Al_2O_3$ (60:30:10).

Source: Sun *et al.* (1997)

Table 1 The activities of catalysts via CO_2 hydrogenation

Catalyst	Reaction Temperature (°C)	CO_2 Conversion (%)	Methanol Selectivity (%)	Methanol Yield (%)
Cu/ZnO (30:70)	220	5.9	47.5	2.8
	240	12.4	31.6	3.6
	260	17.2	19.2	3.3
Cu/ZnO (50:50)	220	7.7	42.8	3.3
	240	13.9	34.5	4.8
	260	18.3	18.6	3.4
Cu/ZnO (60:30)	220	7.2	45.2	3.3
	240	12.2	36.1	4.4
	260	18.2	22.5	4.1
Cu/ZnO/Al_2O_3 (10:80:10)	220	4.6	48.7	2.3
	240	11.1	30.8	3.4
Cu/ZnO/Al_2O_3 (30:60:10)	220	10.4	41.9	4.4
	240	17.0	28.7	4.9
Cu/ZnO/Al_2O_3 (45:45:10)	220	15.5	42.1	6.5
	240	19.3	33.3	6.4
Cu/ZnO/Al_2O_3 (60:30:10)	220	14.7	46.7	6.9
	240	16.8	35.8	6.0
Cu/ZnO/Al_2O_3 (80:10:10)	240	16.1	30.2	4.9

Source: Sun *et al.* (1997)

Jun *et al.* (1998) prepared the Cu/ZnO/Al_2O_3 catalysts to produce methanol from CO_2 hydrogenation and they observed the effect of residual sodium on catalytic activity. The co-precipitation method was used to prepare the Cu/ZnO/Al_2O_3. Copper, zinc, and aluminium nitrates were used to prepare the catalysts (Cu:Zn:Al molar ratio is 1:0.811:0.157). The reactions were operated under 463-523 K and 3 MPa. The

activities of catalysts are shown in Table 2. The most methanol yield can achieve at 523 K and 0 wt% Na-content.

Table 2 The catalyst activities obtained from CO_2 hydrogenation

	Methanol Yield (mol%)				Methanol Selectivity (mol%)			
	Temperature (K)				Temperature (K)			
Catalyst	463	483	503	523	463	483	503	523
$Cu/ZnO/Al_2O_3$ (0wt% Na)	7.4	9.4	10.6	10.6	81.9	66.0	54.7	50.1
$Cu/ZnO/Al_2O_3$ (0.13wt% Na)	5.3	6.2	6.8	7.4	82.0	62.8	45.8	40.1
$Cu/ZnO/Al_2O_3$ (0.18wt% Na)	5	5.6	6	6.6	82.7	64.4	44.2	38.2
$Cu/ZnO/Al_2O_3$ (2.41wt% Na)	0.2	0.2	0.4	0.9	24.5	22.9	16.8	13.4
$Cu/ZnO/Al_2O_3$ (4.18wt% Na)	0	0.1	0.2	0.3	-	15.4	18.0	14.5

Source: Jun *et al.* (1998)

Witoon *et al,* (2013) focused the methanol production via CO_2 hydrogenation over Cu/ZnO catalyst from chitosan-assisted co-precipitation method. The $Cu(NO_3)_2.3H_2O$ and $Zn(NO_3)_2.6H_2O$ (mole ratio of Cu/Zn is 1/1) were used in preparation of Cu/ZnO catalysts. The catalytic activity tests were operated under 453-533 K and 2 MPa. The catalytic activities are shown in Figure 7. The best condition of this study was 513 K and 15.4 m^2/g copper surface area.

Many different kinds of promoters were also used with Cu/Zn based catalyst to produce methanol via CO_2 hydrogenation, such as: ZrO_2 (Guo *et al.,* 2009), SiO_2, TiO_2 (Zhang *et al.,* 2012), carbon nanotubes (CNT) (Dong *et al.,* 2003) (Zhang *et al.,* 2010), and so on. From Dong *et al.*'s and Zhang *et al.*'s works, the CNT resulted in increasing of CO, CO_2 conversion, and methanol formation.

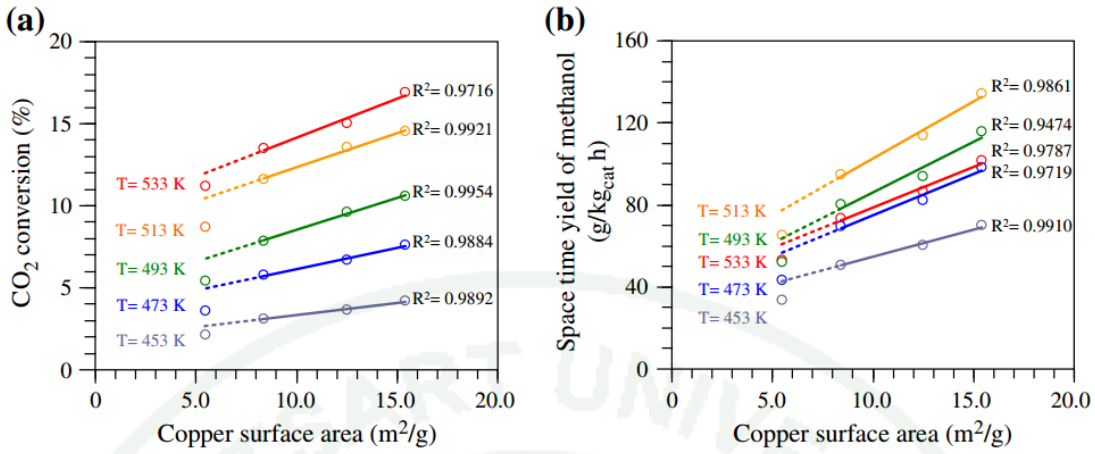

Figure 7 CO_2 conversion (a) and space time yields of methanol (b) at various temperatures and difference copper surface area

Source: Witoon *et al.* (2013)

3. Carbon nanotubes

Carbon nanotubes (CNTs) are nano synthesis material which are different in special structures from the three types of allotropes of carbon (diamond, graphite, and buckminsterfullerenes) as shown in Figure 8. Carbon nanotubes are cylindrical nanostructure which contain carbon molecules. The nanotubes are arranged in hexagonal network.

The chemical bonding of carbon nanotubes is formed as sp^2 with neighboring atoms, similar to graphite. This form means that the 2s-shells and 2p-shells of each carbon atom combine with 2s-shells and 2p-shells of its neighboring atom to form sp^2 bonds. The sp^2 bonding character can be used to approximate the bond in the cylindrical carbon nanotubes and this bonding is stronger than the sp^3 bonds that found in diamond and alkanes. Therefore, carbon nanotubes are provided with the unique strength material. However, the reality carbon nanotubes are not perfect bonding in sp^2 form only. Oftenly, there are defects in the nanotubes which may cause sp^3 bonding. Hence, there is closer approximation is sp^2-sp^3rehybridization. The

different bonding from sp^2 bond is allowed in the cylindrical nature of carbon nanotubes.

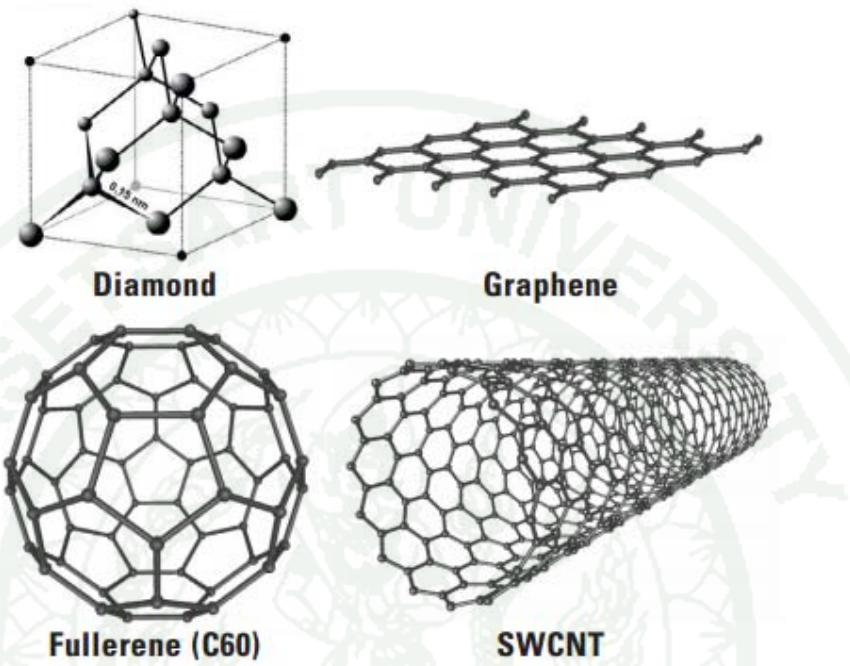

Figure 8 Structure of some representative carbon allotropes.

Source: Hodkiewicz (2010)

The carbon nanotubes are categorized into two types as single-walled carbon nanotubes (SWCNTs) and multi-walled carbon nanotubes (MWCNTs) as shown in Figure 9. The single-walled carbon nanotubes diameter is about 1-2 nm. There are also double-walled carbon nanotubes (DWCNTs) which have a layer of graphene wrapped around the single-walled carbon nanotubes. The double-walled carbon nanotubes are subset of the larger category of multi-walled carbon nanotubes. The multi-walled carbon nanotubes have many layers of graphene wrapped around a core single-walled carbon nanotubes.

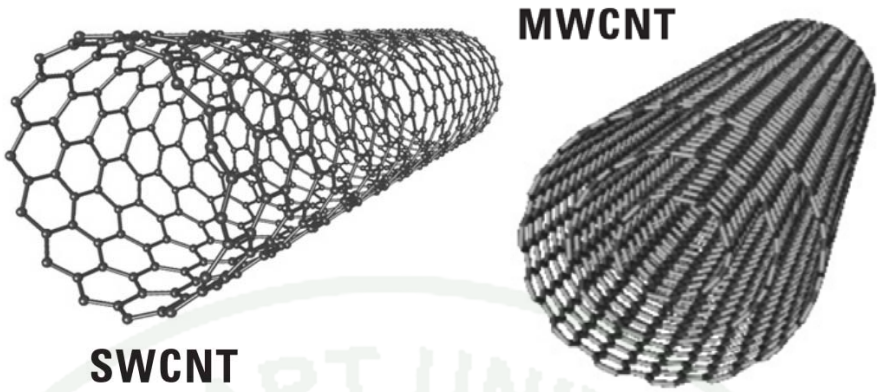

Figure 9 Structure diagrams of carbon nanotubes.

Source: Hodkiewicz (2010)

The carbon nanotubes have many special properties such as high surface area, high thermal stability, chemical inertness, carbon surface chemistry (Rodriguez-Reinoso, 1998), and adsorb and spillover greater amount of hydrogen (Dong *et al.*, 2003) (Chen *et al.,* 2012). The CNTs could induce a metal/support interaction, which attracting increasing attention as novel support for heterogeneous catalysts.

Zhang *et al.,* (2002) did a research on methanol synthesis from $H_2/CO/CO_2$ over CNTs-promoted Cu-ZnO-Al_2O_3 catalyst. The impregnation method was used to prepare the catalysts. The ratio of components in catalyst was studied and the reactions were operated under 463-563 K and 2 MPa. From Figure 10 and Table 3, the optimum temperature in the methanol synthesis of 523-543 K and 32wt%$Cu_6Zn_3Al_1$-O_x/CNTs was the best condition for methanol synthesis in this study.

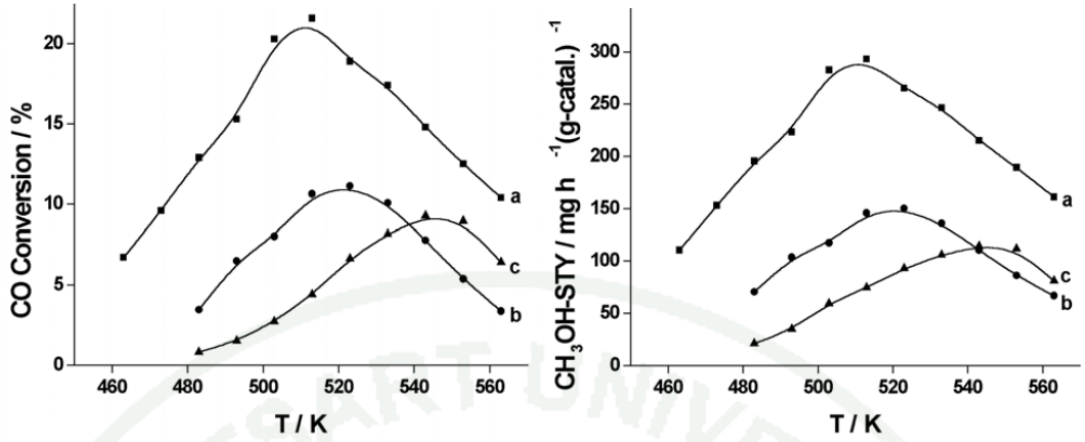

Figure 10 The activities of catalysts (a) 32wt%$Cu_6Zn_3Al_1$-O_x/CNTs, (b) 32wt%$Cu_6Zn_3Al_1$-O_x/AC and (c) 32wt%$Cu_6Zn_3Al_1$-O_x/ɣ-Al_2O_3.

Source: Zhang *et al.,* (2002)

Table 3 Reactivity of methanol synthesis from $H_2/CO/CO_2$ over the catalysts

Catalyst Sample	STY at initiating temperature		STY at the optimum working temperature	
	T/K	STY	T/K	STY
40wt%Cu_5Zn_5-O_x/CNTs	473	55.1	523	182
40wt%Cu_6Zn_3-O_x/CNTs	463	69.3	513	189
40wt%$Cu_{4.5}Zn_{4.5}Al_1$-O_x/CNTs	473	63.4	523	220
40wt%$Cu_5Zn_5Al_{0.5}$-O_x/CNTs	463	49.8	523	232
40wt%$Cu_6Zn_3Al_1$-O_x/CNTs	463	79.4	508	240
42wt%$Cu_6Zn_3Al_1$-O_x/CNTs	473	73.0	523	238
38wt%$Cu_6Zn_3Al_1$-O_x/CNTs	463	101	508	261
32wt%$Cu_6Zn_3Al_1$-O_x/CNTs	463	110	508	287
24wt%$Cu_6Zn_3Al_1$-O_x/CNTs	463	78.4	508	239
32wt%$Cu_6Zn_3Al_1$-O_x/CNTs*	463	100	513	307

* Prepared from ethanol solution of the precursor.

Source: Zhang *et al.* (2002)

Dong *et al.* (2003)studied on synthesis of Cu-ZnO-Al_2O_3 catalyst for methanol synthesis from $H_2/CO/CO_2$. The Cu-ZnO-Al_2O_3 catalysts were prepared from $Cu(NO_3)_2.3H_2O$, $Zn(NO_3)_2.6H_2O$ and $Al(NO_3)_3.9H_2O$ (all AR grades) by co-precipitation method. The reaction was operated under 452-563 K and 2 or 5 MPa. The CO conversion and methanol formation rates are shown in Figure 11. The results showed that the carbon nanotubes affect the rising CO conversion and the methanol formation rate. For the H_2 adsorbability of CNT, H_2-TPD was used to observe the adsorbing of H_2 at the room temperature and 453 K and the results are shown in Figures 12 and 13. The peak in that figures shown desorption on H_2 from CNT.

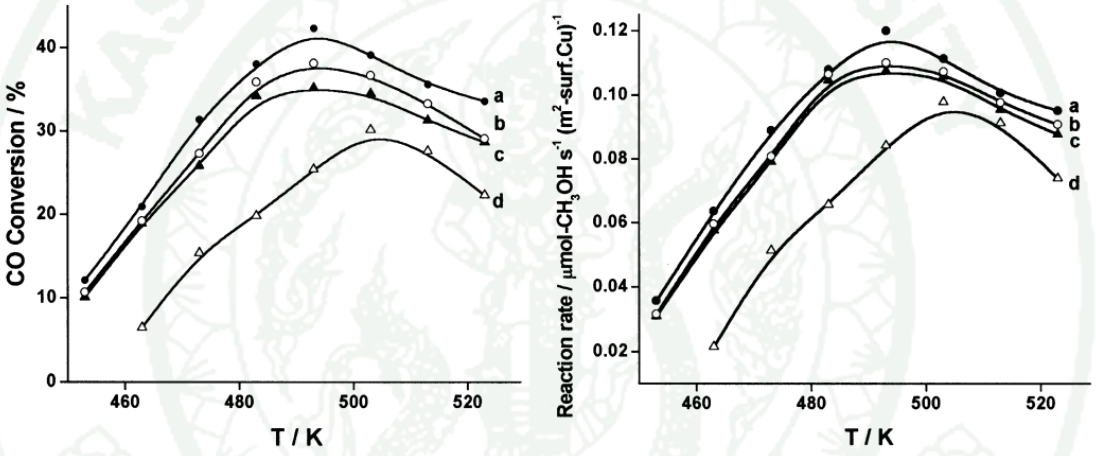

Figure 11 The CO conversion and methanol formation rate on (a) $Cu_6Zn_3Al_1$-12.5%CNTs; (b) $Cu_6Zn_3Al_1$-10%CNTs; (c) $Cu_6Zn_3Al_1$-15%CNTs; (d) $Cu_6Zn_3Al_1$-0%CNTs.

Source: Dong *et al.* (2003)

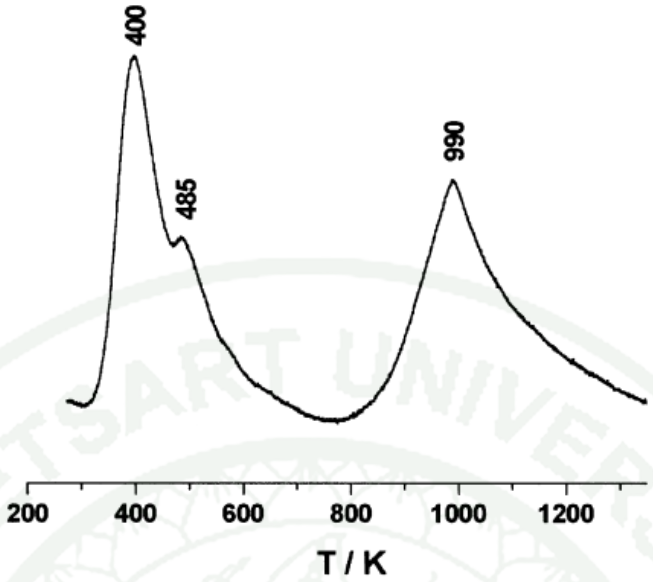

Figure 12 TPD spectrum of H_2 adsorbable on CNT at room temperature.

Source: Dong *et al.* (2003)

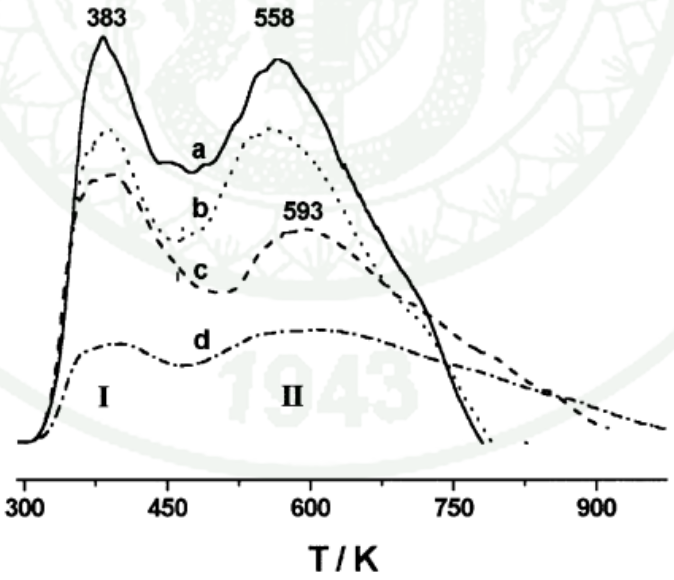

Figure 13 TPD spectrum of H_2 adsorbable on CNT at 453 K.

Source: Dong *et al.* (2003)

Zhang *et al.,* (2010) studied about the methanol and dimethyl ether synthesis over carbon nanotubes intercrossed Cu/Zn/Al/Zr catalyst via CO/CO_2 hydrogenation. The catalysts were prepared by co-precipitation method using $Cu(NO_3)_2.6H_2O$, $Zn(NO_3)_2.6H_2O$, $Al(NO_3)_3.6H_2O$, and $ZrOCl_2$ with a ratio of 6:3:0.5:0.5. The CO_2 hydrogenation in this study was operated under 230(CO)/240(CO_2) ºC and 4 MPa. The catalyst activities are shown in Table 4. The CO_2 conversion of CD703 catalyst was more than COM and CD503 catalyst. Also, the STY showed similar trend to the conversion.

Table 4 The conversion and space time yield (STY) of the catalysts

Catalyst	CO_2 hydrogenation	
	CO_2 conversion	STY, g/(gcat h)
COM*	0.163	0.151
CD503**	0.205	0.261
CD703***	0.215	0.282

* COM is commercial catalyst ($Cu/ZnO/Al_2O_3$).

** CD503 is Cu/Zn/Al/Zr catalyst.

*** CD703 is long CNT intercrossed Cu/Zn/Al/Zr catalyst.

Source: Zhang *et al.* (2010)

4. The Surface functionalization of carbon nanotubes

Normally, carbon nanotubes have many kinds of nanotubes mixture and impurities (Yudianti *et al.*, 2011). Functionalization of carbon nanotubes affects density of defect on carbon nanotube surface. Yudianti *et al.* studied the functional group on multi-walled carbon nanotubes surface. In their study, carbon nanotubes were treated by low concentration of nitric acid solution. They found that the carbon nanotubes surface had some particle impurities attached onto its surface. After acid treatment, the impurities were removed from the surface and the layer of carbon nanotubes became thinner because erosion and fiber was shorter due to cutting. The

strong acid solution was used in the functionalization process. According to the process, oxygenated acidic group was occurred on the surface of carbon nanotubes and open-ended pipes.

This study focused on production methanol over CuO/ZnO/functionalized CNT catalysts via CO_2 hydrogenation. The co-precipitation method was used to prepare the catalysts. The catalysts were tested for their activities under 220-280 ºC and 3 MPa in fixed-bed reactor. The ratio of Cu/Zn/CNT, types of acid used in functionalization step and temperature variation were recorded.

MATERIALS AND METHODS

1. Materials and Equipment

1.1 Multi-walled carbon nanotubes (purchased from Bayer, 95% purified, outside and inside diameter are about 13 and 4 nm; respectively, length is more than μm)

1.2 Sulfuric acid: H_2SO_4 98% (AR grade purchased from Qrec)

1.3 Nitric acid: HNO_3 65% (AR grade purchased from CARLO ERBA)

1.4 Phosphoric acid: H_3PO_4 85% (AR grade purchased from Univar)

1.5 $Cu(NO_3)_2.3H_2O$ (AR grade)

1.6 $Zn(NO_3)_2.6H_2O$ (AR grade)

1.7 $NaHCO_3$ (AR grade)

1.8 N_2 adsorption/desorption (Quantachrome Instruments, NOVA 2000e)

1.9 Fourier Transform Infrared (FTIR : Thermo Scientific, Nicolet 6700)

1.10 Raman Spectroscopy (NTEGA spectro, NT-MDT)

1.11 Scanning Electron Microscopy (SEM : JEOL JSM-7600F)

1.12 Transmission Electron Microscopy (TEM : JEOL JEM-2010)

1.13 X-Ray Diffraction (XRD : Bruker, D8 Advance)

1.14 Thermal Conductivity Detector (TCD) (Varian 4800, alltech 8700 column)

1.15 Flame Ionization Detector (FID) (Shimadzu GC-8A, porapak q column)

2. Methodology

2.1 Funtionalization step

Figure 14 shows functionalization step, three (3) grams of multi-walled carbon nanotubes were added into 150 milli-litres of acid solution. The carbon nanotubes in acid solution were sonicated for 2 hours and upheld for 18 hours. Then, sample was filtered and dried in air at 100 ^{o}C for 16 hours.

Acid solution

- H_2SO_4 150 milli-litres
- HNO_3 150 milli-litres
- H_3PO_4 150 milli-litres

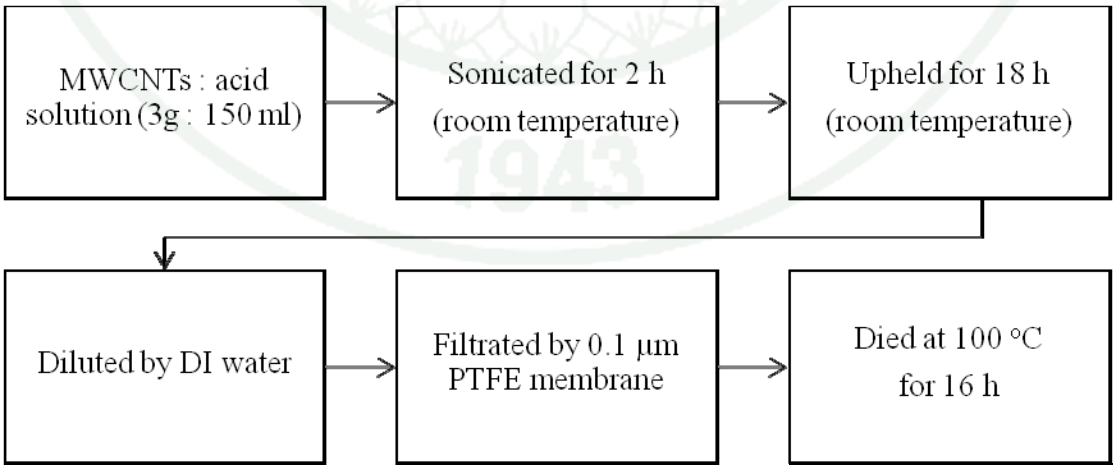

Figure 14 Functionalization step of functionalized MWCNTs

2.2 Co-precipitation step

Co-precipitation step of catalysts showed in Figure 15. $Cu(NO_3)_2.3H_2O$ and $Zn(NO_3)_2.6H_2O$ were diluted in 100 milli-litres DI water. Then, the MWCNTs were added into that solution and stirred for 10 minutes. 100 milli-litres of 0.1 M $NaHCO_3$ were dropwise added to that solution and stirred for 2 hours. On stirring, pH was controlled to be around 7-8 with 0.1 M $NaHCO_3$. After that, sample was filtered and washed with DI water. Then, sample was washed again with ethanol solution. The catalyst sample was dried in air at 100 ºC for 16 hours. Lastly, sample was calcined at 350 ºC for 4 hours in air.

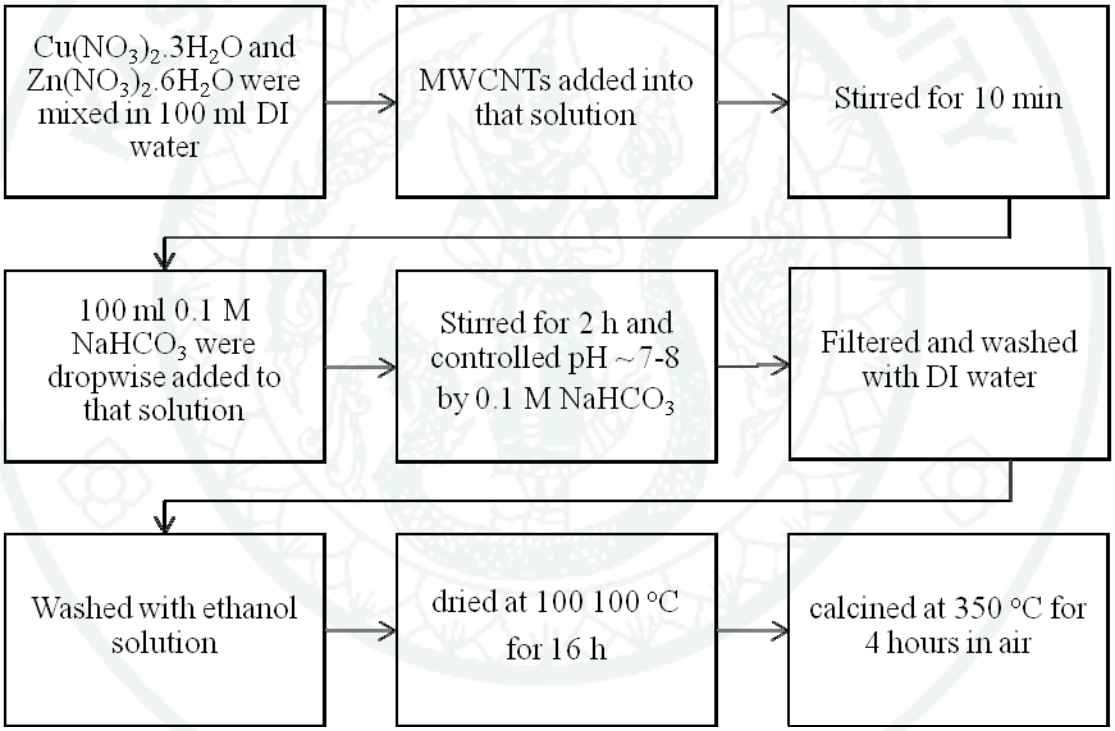

Figure 15 Co-precipitation step of catalysts

2.3 Reaction step

The CO_2 hydrogenation was carried out in a stainless steel fixed-bed reactor. 0.5 grams of catalyst mixed with 0.5 grams of sea sand were added into reactor. Before reaction testing, the catalyst was preheated with pure Argon (Ar) flow at 300 ºC. The catalyst was reduced immediately for 4 hours in pure H_2 flow at the

same temperature. Then, 25 % of CO_2 and 75 % of H_2 mixed gases were allowed to flow to the fixed-bed reactor. The product was analyzed by gas chromatography (GC) with a thermal conductivity detector and a flame ionization detector. Helium gas (He) was used as a carrier gas for the gas chromatography.

RESULTS AND DISCUSSION

This part describes the results with discussion about the methanol production via CO_2 hydrogenation over CuO/ZnO/MWCNTs catalysts. The results and discussion are divided into three sections: characterization of CuO/ZnO/MWCNTs catalysts, characterization of acid functionalized MWCNTs, and characterization of functionalized MWCNTs added into CuO/ZnO catalysts.

1. Characterization and catalytic performances of CuO/ZnO/MWCNTs catalysts

1.1 Characterization of CuO/ZnO/MWCNTs catalysts

The CuO/ZnO/MWCNTs catalysts were characterized by N_2-sorption, X-Ray Diffraction (XRD), Temperature Program Reduction (TPR), N_2O chemisorption, Scanning Electron Microscopy (SEM), and Transmission Electron Microscopy (SEM). Table 5 showed the BET surface area, total pore volume, pore diameter of the CuO/ZnO/MWCNTs catalysts.

The BET surface area and total pore volume of the catalyst prepared in the absence of MWCNTs were found to be 47.80 m^2/g and 0.13 cm^3/g, respectively. The pristine multiwall carbon nanotubes (MWCNTs) had the BET surface area and total pore volume of 136.40 m^2/g and 0.42 cm^3/g, respectively. The catalysts were prepared with the contents of MWCNTs (20-40 wt%) exhibited a drastic reduction and the 60-80 wt% MWCNTs contents showed doubling increasing in both BET surface area and total pore volume when compared to those of the MWCNTs-free catalyst. This could be explained by the fact that the CuO and ZnO particles deposited on the MWCNTs (20-40 wt%) and also blocked the pores. But CuO and ZnO particles could be well dispersed on the 60-80 wt% MWCNTs contents catalysts. This could be confirmed by SEM images. The MWCNTs ratio variation did not really affect to the average pore diameter of the catalysts.

Table 5 BET surface area, total pore volume, and pore diameter of the CuO/ZnO/ MWCNTs catalysts

Catalyst	BET surface area (m^2/g)	Total pore volume (cm^3/g)	Pore diameter (nm)
50/50 CuO/ZnO	47.80	0.13	3.63
40/40/20 CuO/ZnO/MWCNTs	15.22	0.04	3.64
30/30/40 CuO/ZnO/MWCNTs	21.18	0.04	3.25
20/20/60 CuO/ZnO/MWCNTs	104.50	0.37	3.64
10/10/80 CuO/ZnO/MWCNTs	120.20	0.39	3.25
MWCNTs	136.40	0.42	3.25

The metallic copper surface areas, dispersion and Cu particle size of the CuO/ZnO/MWCNTs catalysts which were analyzed using N_2O chemisorption method are shown in Table 6. The metallic copper surface area of the MWCNTs-free catalyst is 3.45 m^2/g cat. The catalysts which was prepared with 20-80 wt% MWCNTs contents demonstrated reduction of metallic copper surface area. The dispersion of the MWCNTs-free catalyst is 0.75 percent. The 20-80 wt% MWCNTs contents catalysts have lower dispersion than that of the MWCNTs-free catalyst. The Cu particle size of the MWCNTs-free catalysts is about 97.5 nm. The 20-40 wt% MWCNTs contents catalysts have bigger Cu particle size and 60-80 wt% MWCNTs contents catalyst have smaller Cu particle size than that of the MWCNTs-free catalyst. This results could be confirmed by SEM and TEM observation.

Table 6 The metallic copper surface area, dispersion and Cu particle size of CuO/ZnO/MWCNTs catalysts

Catalyst	Metallic copper surface area (m^2/g cat)	Dispersion (%)	Cu particle size(nm)
50/50 CuO/ZnO	3.45	0.75	97.48
40/40/20 CuO/ZnO/MWCNTs	1.43	0.31	188.55
30/30/40 CuO/ZnO/MWCNTs	1.29	0.27	157.0
20/20/60 CuO/ZnO/MWCNTs	1.89	0.41	71.37
10/10/80 CuO/ZnO/MWCNTs	1.15	0.25	58.38

The SEM morphologies of CuO/ZnO/MWCNTs catalysts are shown in Figure 16. For the catalyst without MWCNTs addition, the CuO and ZnO particles were agglomerated. As well as the N_2O chemisorption result, the particle sizes of catalysts which were prepared with 20-40 wt% MWCNTs contents are bigger and the dispersion is lower than the catalyst without MWCNTs. On the other hand, the catalysts with 60-80 wt% MWCNTs contents represented well CuO and ZnO particles dispersion on MWCNTs and the particles that decorated on MWCNTs were smaller than the MWCNTs-free catalysts. Figure 16b and 16c could confirm the BET surface areas and total pore volume results of the CuO and ZnO particles deposited on the MWCNTs (20-40 wt% contents), blocked the pore, and affected bigger particle size.

The TEM observations are shown in Figure 17. The MWCNTs-free catalyst represented agglomeration of CuO and ZnO particles. The addition of MWCNTs to the CuO/ZnO catalyst with 20-40 wt% contents affected bigger particles size and lower dispersion of CuO and ZnO. On the other hand, the higher MWCNTs addition with 60-80 wt% contents effected the smaller particle size and well dispersion of CuO and ZnO on MWCNTs.

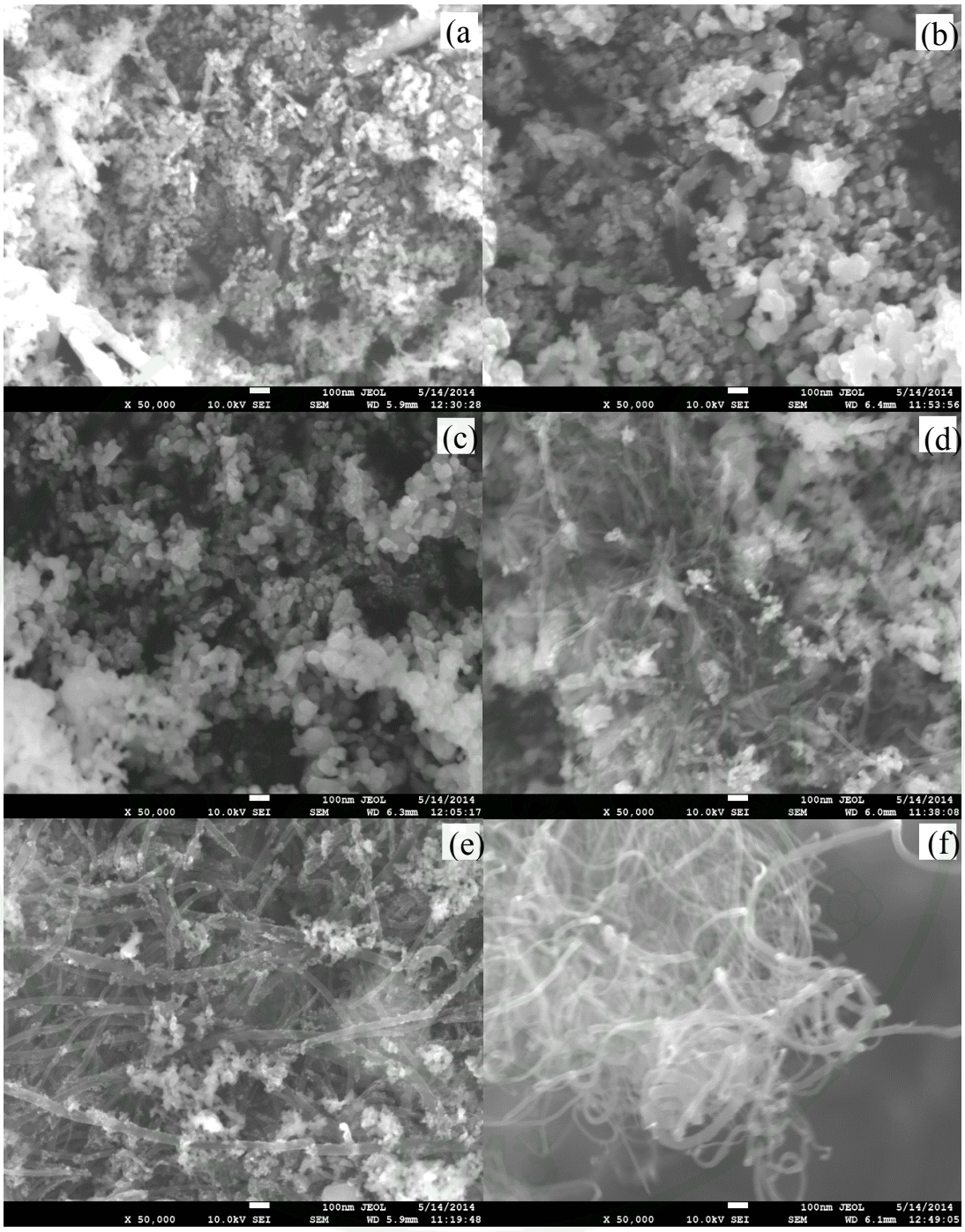

Figure 16 Scanning electron microscope images of 50/50 CuO/ZnO (a), 40/40/20 CuO/ZnO/MWCNTs (b), 30/30/40 CuO/ZnO/MWCNTs (c), 20/20/60 CuO/ZnO/MWCNTs (d), 10/10/80 CuO/ZnO/MWCNTs (e) and pristine MWCNTs (f)

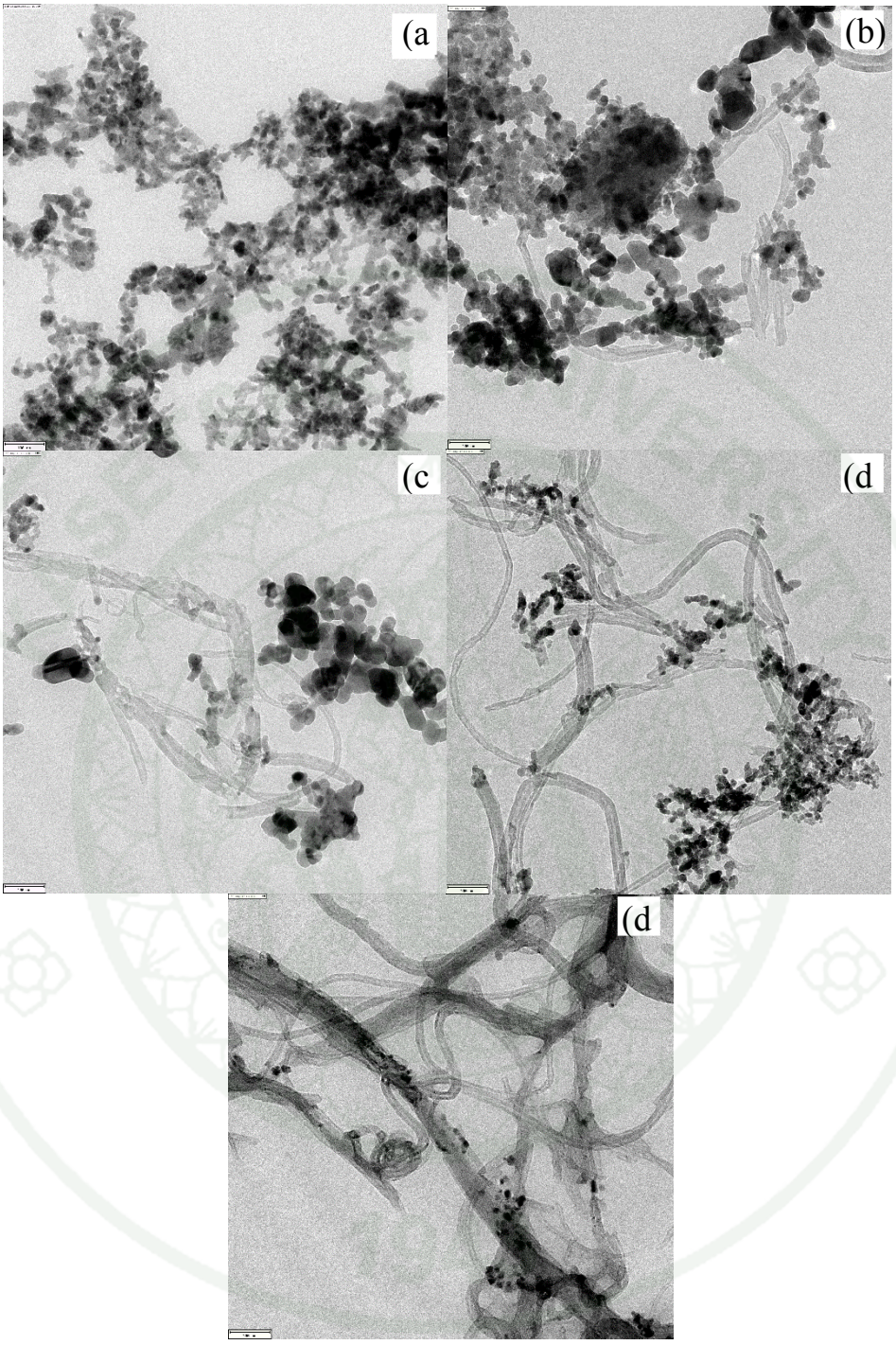

Figure 17 Transmission electron microscope images of 50/50 CuO/ZnO (a), 40/40/20 CuO/ZnO/MWCNTs (b), 30/30/40 CuO/ZnO/MWCNTs (c), 20/20/60 CuO/ZnO/MWCNTs (d), and 10/10/80 CuO/ZnO/MWCNTs (e)

The XRD patterns of the CuO/ZnO/MWCNTs powder catalysts are shown in Figure 18. The XRD patterns of all catalysts showed the same peak pattern of CuO and ZnO. But the MWCNTs added to CuO/ZnO catalysts showed another peak that was MWCNTs' peak. The copper oxide (CuO) monoclinic phase was observed at 2θ of 35.5º, 38.7º 48.7º, 61.5º, and 66.2º corresponding to (-1 1 1), (1 1 1), (-2 0 2), (2 0 2), (-1 1 3) and (-3 1 1) crystal planes, respectively. The hexagonal zinc oxide (ZnO) was observed at 31.8º, 34.5º, 36.3º, 47.7º, 56.7º, 63.0º, and 68.1º which was correspondent to the crystal planes (1 0 0), (0 0 2), (1 0 1), (1 0 2), (1 1 0), (1 0 3), and (1 1 2), respectively. The peak of MWCNTs appeared at 26º and 43º corresponding to the crystal planes (0 0 2). The CuO and ZnO crystal sizes of the catalysts that calculated at 38.4º and 31.8º are shown in Table 7. The CuO and ZnO crystal sizes of MWCNTs-free catalyst were 12.9 and 14.8 nm, respectively. The 20-40 wt% MWCNTs contents catalysts showed double increasing of both crystal sizes. But the CuO and ZnO crystal sizes of the 60-80 wt% MWCNTs contents catalysts were not significantly different from those of the MWCNTs free catalyst.

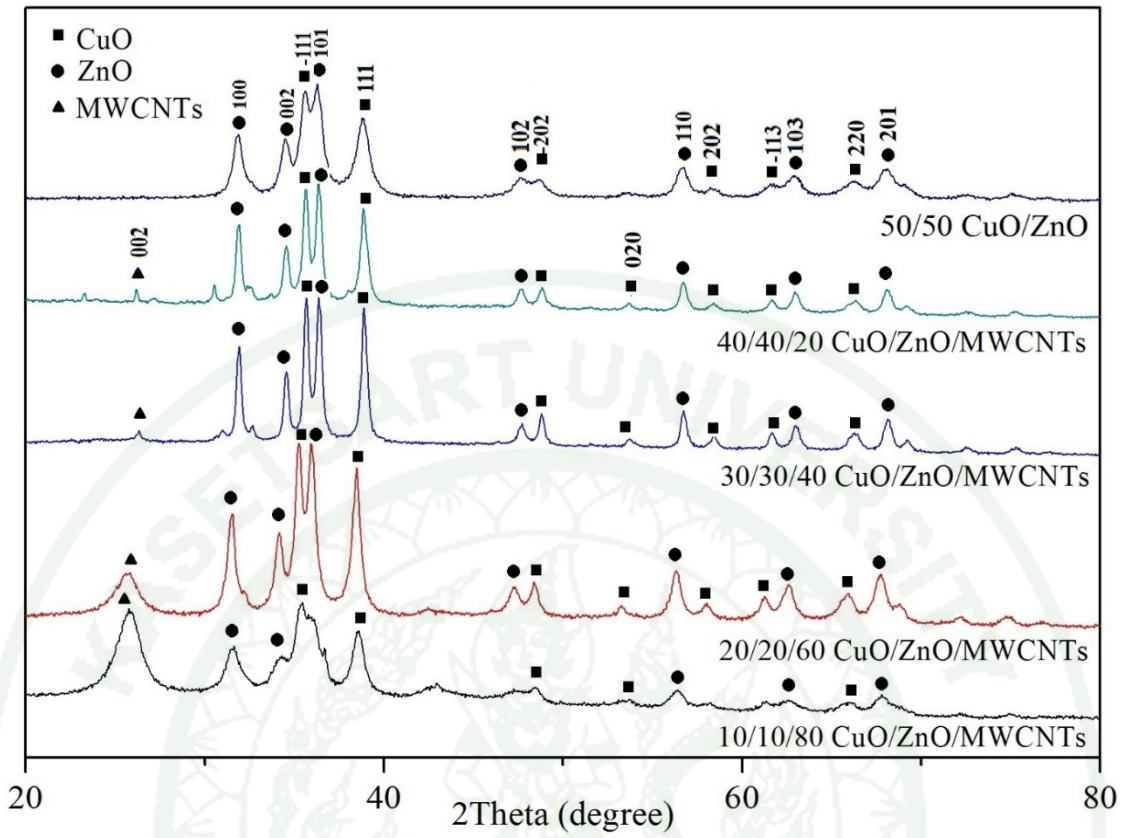

Figure 18 X-ray diffraction spectra of catalysts

Table 7 The CuO and ZnO crystal sizes of catalysts

Catalyst	CuO crystal size (nm)	ZnO crystal size (nm)
50/50 CuO/ZnO	12.89	14.82
40/40/20 CuO/ZnO/MWCNTs	21.38	29.53
30/30/40 CuO/ZnO/MWCNTs	25.91	30.67
20/20/60 CuO/ZnO/MWCNTs	19.12	18.70
10/10/80 CuO/ZnO/MWCNTs	13.84	11.51

The reducibility of catalysts shown in Figure 19 was observed using H_2-temperature program reduction (H_2-TPR). The catalyst without MWCNTs represented the reduction temperature of about 220-340 °C. The 20 wt% the MWCNTs contents addition affected the reducing in temperature higher than MWCNTs-free catalyst and showed the temperature range of about 260-390 °C. The reducibility of 40 wt% MWCNTs contents catalyst represented in a temperature range of about 260-370 °C. The 60 wt% MWCNTs addition affected in lower range of the catalyst reduction temperature of about 180-340 °C. The reduction temperature of 80 wt% MWCNTs contents addition showed a range of about 160-280 °C. Rhodes and Bell (2005) attributed that the lower reduction temperature resulted in reduction of highly dispersion of CuO, while the higher reduction temperature caused reduction of the CuO bulk. The 60-80 wt% MWCNTs contents effected lowering in reduction temperature than the catalysts without MWCNTs. The dispersion of CuO particles could be observed by scanning and transmission electron microscopes as shown in Figure 16-17.

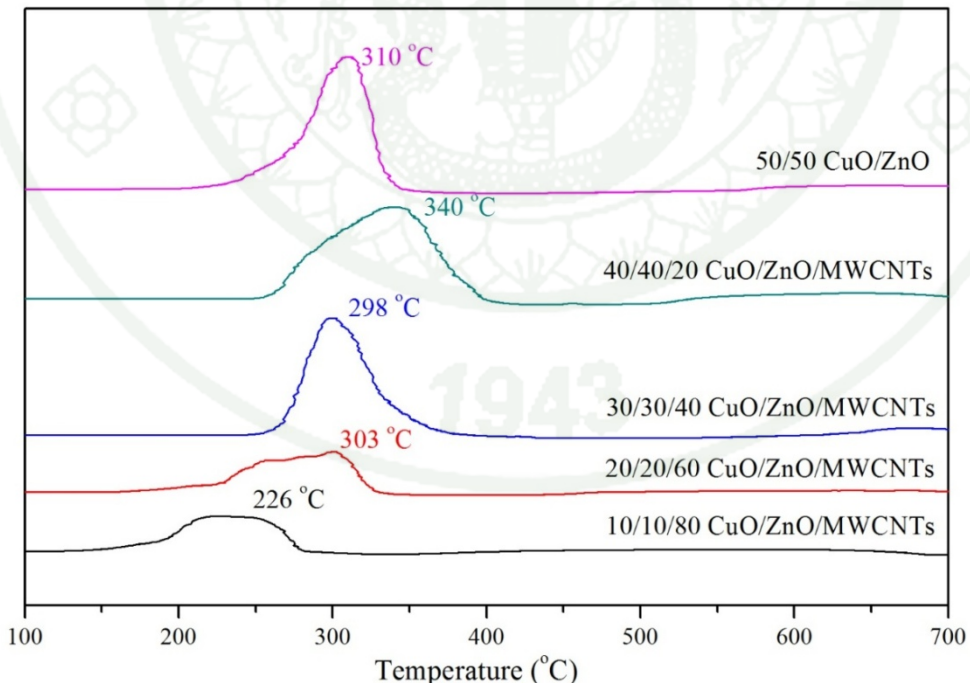

Figure 19 H_2-Temperature program reduction spectra of catalysts

1.2 Catalytic performance of CuO/ZnO/MWCNTs catalysts

Catalytic performance of CuO/ZnO/MWCNTs catalysts were investigated during the process of carbondioxide hydrogenation to be methanol. The reaction was performed in a fixed bed reactor using CO_2/H_2 gas feed ratio of 3:1 and 30 bar absolute pressure. The reaction temperatures were studied at 220, 250, and 280 ^oC. Every single catalyst was given its specific name following its ratio (Table 8).

As a function of reaction temperature, CO_2 conversion and methanol selectivity of the CuO/ZnO/MWCNTs catalysts are shown in Figure 20 and Figure 21, respectively. Typically, the CO_2 conversion increased with increasing of reaction temperature. The catalyst without MWCNTs exhibited the highest CO_2 conversion at 250 and 280 ^oC of about 17 and 25 percent, respectively, while the 60 wt% MWCNTs contents catalyst showed the highest CO_2 conversion at 220 ^oC of 8 percent. For the metallic copper surface area of the catalysts as determined from N_2O chemisorption, the catalysts without MWCNTs showed the highest copper metallic surface area. For methanol selectivity, it was decreased with the increasing of reaction temperature while the CO selectivity incresed with increasing reaction temperature (Figure 22). The increasing of reaction temperature affected in decreasing of methanol selectivity because the methanol synthesis was the exothermic reaction. However, the CO selectivity increased because the reverse water-gas shift reaction was the endothermic reaction. The 80 wt% MWCNTs contents catalyst exhibited the highest methanol selectivity of about 35, 27, and 15 percent with 220, 250 and 280 ^oC reaction temperature, respectively. The catalyst without MWCNTs showed the almost lowest methanol selectivity in all reaction temperatures but high CO selectivity than the other catalysts. The methanol space time yield increased with the reaction temperature increasing (Figure 23). The 60 wt% MWCNTs contents catalyst exhibited the highest methanol space time yield about 44, 51, and 58 $g_{methanol}/(kg_{catalyst}\ h)$ at 220, 250 and 280 ^oC, respectively. Hence, the 60 wt% MWCNTs contents catalyst was chosen for preparing of the catalysts with functionalized MWCNTs.

Table 8 Specified name of CuO/ZnO/MWCNTs catalysts

Catalyst	Specific name
50/50 CuO/ZnO	50/50
40/40/20 CuO/ZnO/MWCNTs	40/40/20
30/30/40 CuO/ZnO/MWCNTs	30/30/40
20/20/60 CuO/ZnO/MWCNTs	20/20/60
10/10/80 CuO/ZnO/MWCNTs	10/10/80

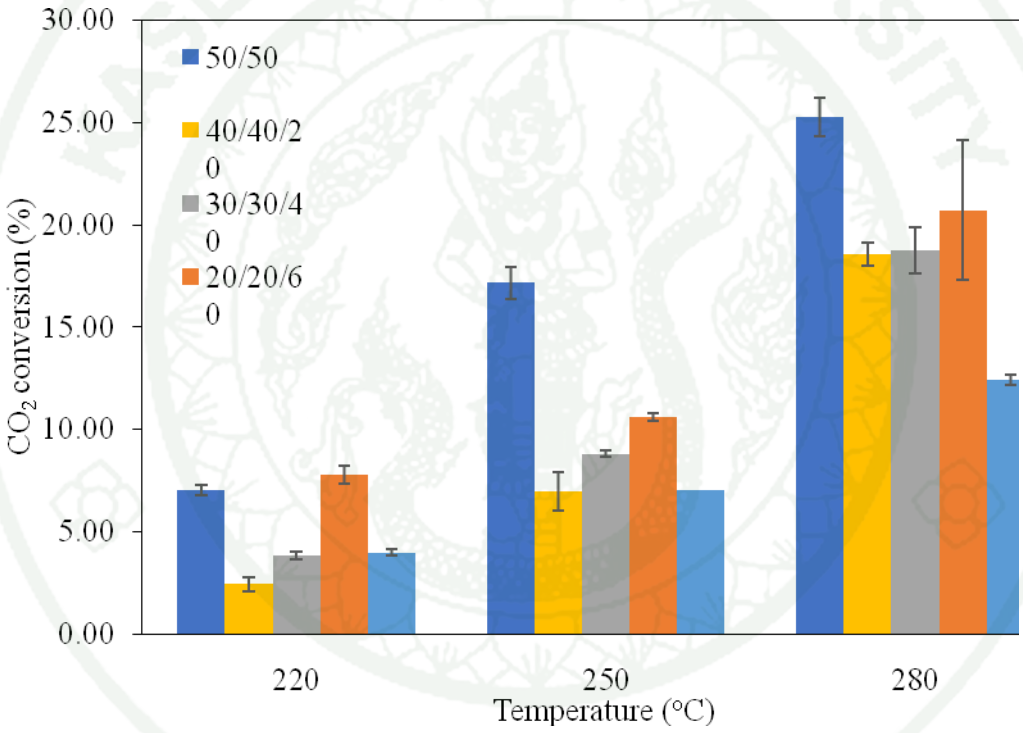

Figure 20 CO_2 conversion of CuO/ZnO/MWCNTs catalysts

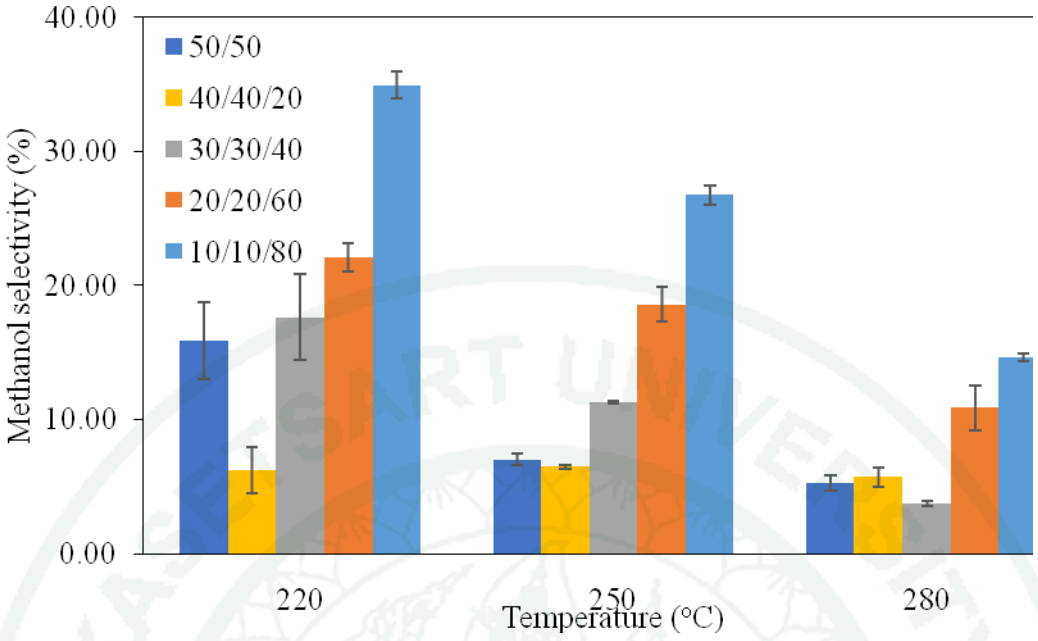

Figure 21 Methanol selectivity of CuO/ZnO/MWCNTs catalysts

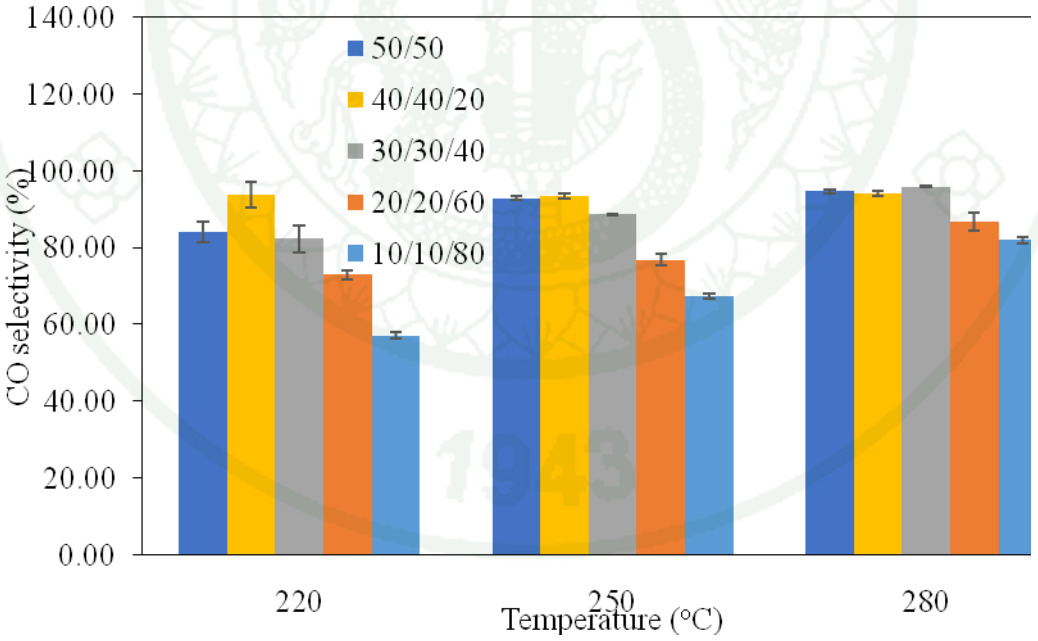

Figure 22 CO selectivity of CuO/ZnO/MWCNTs catalysts

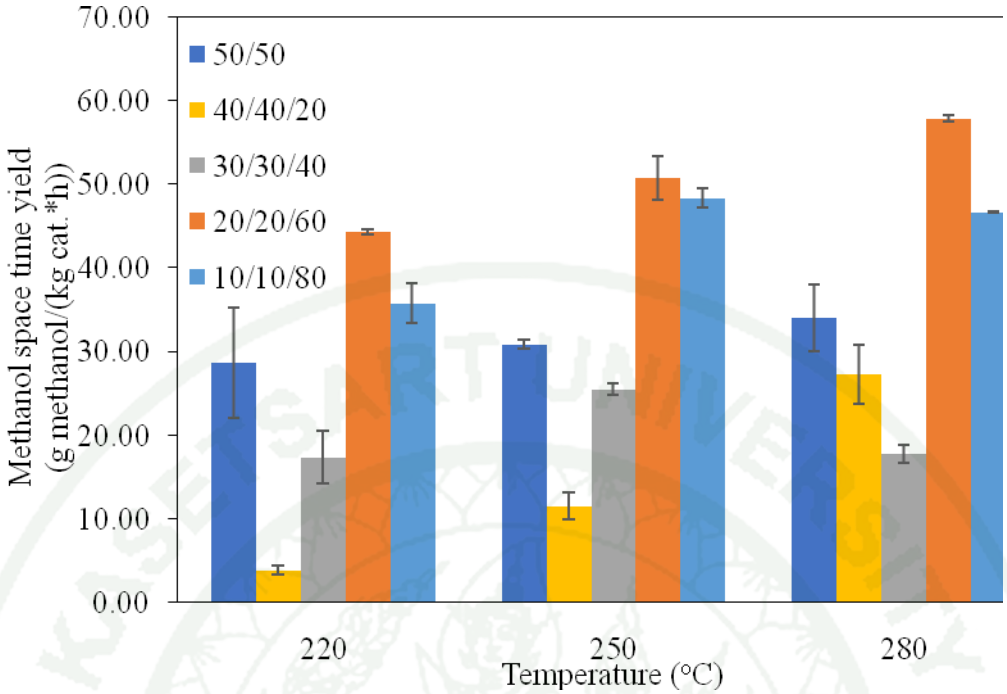

Figure 23 Methanol space time yield of CuO/ZnO/MWCNTs catalysts

2. Characterization of functionalized MWCNTs

The MWCNTs were functionalized by acid solution. List of acid solution is shown in Table 9. The functionalized MWCNTs were characterized by N_2 adsorption/desorption, Raman spectroscopy, and the mid-infrared range Fourier transform spectroscopy (FT-IR).

The BET surface area, pore volume, and pore diameter of pristine and functionalized carbon nanotubes are shown in Table 10. The BET surface area and pore volume of pristine carbon nanotubes were found to be 136.4 m^2/g and 0.42 cm^3/g, respectively. After acid treatment, those properties were found to be significantly increased, and strongly depended on types of acid. This could be potentially explained by the fact that the strong acid could open up the end of the tubes and create more defect formation on the side wall. Increasing of intensity ratio (I_D/I_G) from Raman spectroscopy could confirm the defect on the site wall of

functionalized carbon nanotubes (Table 11). It is worth to note that the acid treatment did not affect the pore diameter.

Table 9 Acid solution and identified name of functionalized MWCNTs

Acid solution	Specify name
-	MWCNTs
H_2SO_4 (98% purity)	s-MWCNTs
HNO_3 (65% purity)	n-MWCNTs
H_3PO_4 (85% purity)	p-MWCNTs

Table 10 Textural and structure properties

Catalyst Sample	Surface area (m^2/g)	Pore volume (cm^3/g)	Pore diameter (nm)
MWCNTs	136.40	0.42	3.25
s-MWCNTs	156.50	0.67	3.25
n-MWCNTs	138.30	0.54	3.25
p-MWCNTs	146.10	0.66	3.25

Table 11 The intensity ratio of Raman spectral

Catalyst Sample	I_D/I_G
MWCNTs	1.103
s-MWCNTs	1.182
n-MWCNTs	1.118
p-MWCNTs	1.227

The Raman spectra of pristine and functionalized MWCNTs are shown in Figure 24. The D band (~1323 cm-1) and D' band (~1605 cm-1) were related to the defection of sp^3-hybridizes carbons and disorder of structure on MWCNTs (Ma *et al.,* 2010; Shao *ei al.,* 2010; Yang *wt al.,* 2010; and Hooijdonk *et al.,* 2013), while the G band was related to the graphite structure of MWCNTs (sp^2-hybridizes carbon atom of carbon nanotubes). The intensity ratio of D and G band (I_D/I_G) was used to estimate the disordering and defect presented on the wall of MWCNTs (Osswaled *et al.,* 2007).

As shown in Table 11, the intensity ratio of functionalized MWCNTs were more than that of pristine MWCNTs. Phosphoric acid solution (H_3PO_4) made more defection on the wall of MWCNTs than the sulfuric (H_2SO_4) and nitric (HNO_3) acid solution.

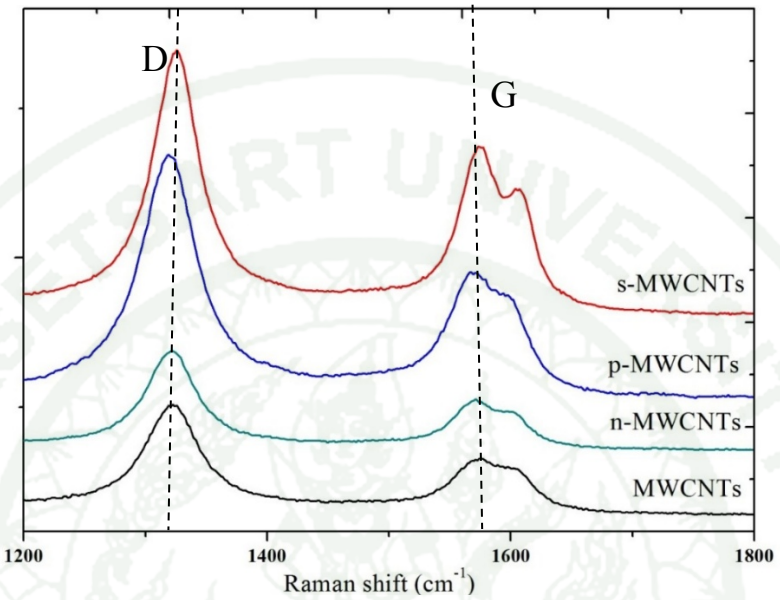

Figure 24 Raman spectra of pristine carbon nanotubes and functionalized carbon nanotubes

Functional groups on pristine and functionalized MWCNTs were characterized by the mid-infrared range Fourier transform spectroscopy (FT-IR) that showed in Figure 25. The frequency range was observed in a range of 4,000-400 cm^{-1}. The absorbance band at ~1,719 cm^{-1} can describable to carbonyl (C=O) stretching vibration of carboxyl group on the side wall of MWCNTs. The C-O, C=C, C-H bond and hydroxyl groups (OH) appeared at ~1,368 , ~1,587 , ~2,900 , and ~3,341 cm^{-1}, respectively (Naseh *et al.,* 2009 and Yudianti *et al.,* 2011). The carboxylic group (COOH) was formed from oxidation of C-O, C=O, O-H bond (Her *et al.,* 2013).

To this section, the functionalized MWCNTs which resulted more defects were sulfuric and phosphoric acid solution. Hence, both kinds of acid solution were chosen to prepare the catalysts with functionalized MWCNTs.

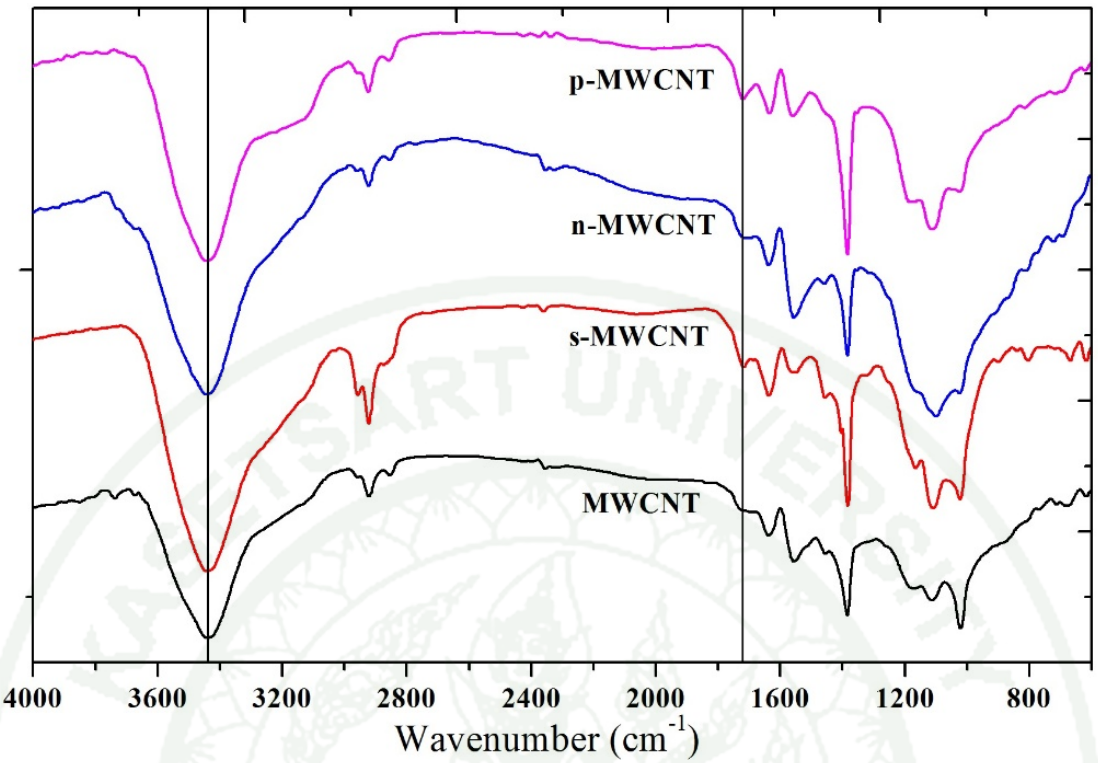

Figure 25 FT-IR spectra of pristine and functionalized MWCNTs

3. Characterization and catalytic performance of the functionalized MWCNTs

3.1 Characterization of CuO/ZnO/MWCNTs catalysts

With reference to the previous section, the 60 wt% MWCNTs contents catalyst showed the highest performance in the methanol synthesis and the functionalized MWCNTs with sulfuric and phosphoric acid solution represented defects on the wall of MWCNTs. Thus, the 60 wt% MWCNTs contents were used to prepare the catalysts with the functionalized MWCNTs. The functionalized MWCNTs with added CuO/ZnO catalysts were characterized using N_2-sorption, X-Ray diffraction (XRD), temperature program reduction (TPR), N_2O chemisorption, scanning electron microscopy (SEM), and transmission electron microscopy (TEM).

The N_2-sorption was used to observe the BET surface area, total pore volume, and total pore diameter of the catalysts. Regarding the previous section, the

BET surface area and total pore volume of the pristine MWCNTs catalyst were found to be 104.50 m^2/g and 0.37 cm^3/g, respectively. The catalysts with functionalized MWCNTs showed more BET surface area than the catalyst with MWCNTs. This could be confirmed by the BET resulted from the functionalized MWCNTs section that the functionalized MWCNTs had more BET surface area than the pristine one. However, the total pore volume and pore diameter of the functionalized MWCNTs catalyst were not significantly different with the catalyst with pristine MWCNTs (Table 12).

Table 12 BET surface area, total pore volume, and pore diameter of the functionalized MWCNTs added into CuO/ZnO catalysts

Catalyst	BET surface area (m^2/g)	Total pore volume (cm^3/g)	Pore diameter (nm)
20/20/60 CuO/ZnO/MWCNTs	104.50	0.37	3.64
20/20/60 CuO/ZnO/s-MWCNTs	124.59	0.40	3.25
20/20/60 CuO/ZnO/p-MWCNTs	111.90	0.49	3.24

Table 13 showed the metallic copper surface area, dispersion and Cu particle size of the pristine and functionalized MWCNTs catalysts by using N_2O chemisorption method. Again, the previous section described that the metallic copper surface area of the pristine MWCNTs catalyst is about 1.89 m^2/g cat. The functionalized MWCNTs catalysts exhibite about 3.98 and 3.62 m^2/g cat of metallic copper surface area of sulfuric and phosphoric functionalized MWCNTs catalysts, respectively. Likewise, the dispersion of functionalized MWCNTs catalysts ishigher than that of the pristine MWCNTs. However, the dispersion of both acid functionalized MWCNTs catalysts is not significantly difference.The Cu particle size of the pristine MWCNTs catalyst is about 71.4 nm. The functionalized MWCNTs catalysts have smaller Cu particle size than that of the pristine one.From the previous section, the defect of functionalized MWCNTs surface might be cause of increasing of methallic copper surface area and dispersion, and reduction of Cu particle size.

This results could be explianed by the XRD, SEM, and TEM images which showed the cyrstal size of CuO, ZnO, and dispersion of the catalysts particles.

Table 13 The metallic copper surface area, percent dispersion and Cu particle size of the functionalized MWCNTs added into CuO/ZnO catalysts

Catalyst	Metallic copper surface area (m^2/g cat)	Dispersion (%)	Cu particle size (nm)
20/20/60 CuO/ZnO/MWCNTs	1.89	0.41	71.38
20/20/60 CuO/ZnO/s-MWCNTs	3.98	0.76	38.34
20/20/60 CuO/ZnO/p-MWCNTs	3.62	0.79	37.19

Morphology of the pristine and functionalized MWCNTs catalysts prepared by co-precipitation method were observed by SEM (Figure 24). Without functionalization, the catalyst particles would have bigger size and higher dispersion than that of the functionalized MWCNTs and this could beclearly confirmed by TEM images.

As shown by the TEM images in Figure 27, the CuO and ZnO particles were decorated on the pristine and functionalized MWCNTs. The sulfuric functionalized MWCNTs represented smaller particles size than the others (Figure 25b). As well as the dispersion and metal particle size from N_2O chemisorption method, the catalyst with functionalized MWCNTs revealed better dispersion and smaller CuO and ZnO particles than the catalyst with pristine MWCNTs. This could be concluded that the defections of MWCNTs surface affected the dispersion of CuO and ZnO particles on the wall of functionalized MWCNTs.

Reducibility of the MWCNTs and functionalized MWCNTs catalysts are shown in Figure 28. The pristine MWCNTs catalyst exhibited range of reduction temperature between 180-340 ^oC. Meanwhile, the functionalized MWCNTs catalyst showed a bit lower range of 180-330 ^oC. The reducibility of the catalysts with pristine and functionalized MWCNTs contents were not significantly different.

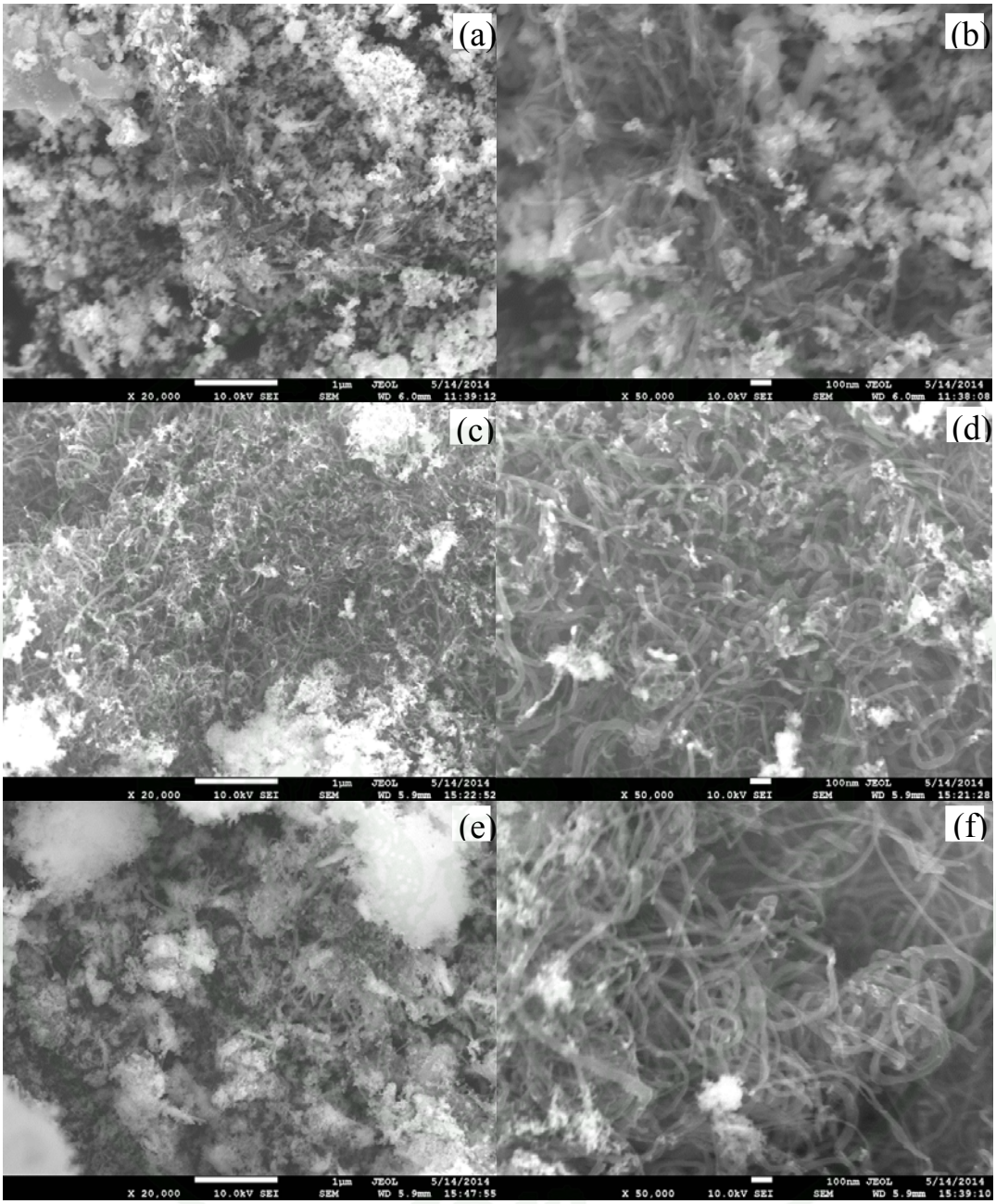

Figure 26 Scanning electron microscope images of 20/20/60 CuO/ZnO/MWCNTs (a) and (b), 20/20/60 CuO/ZnO/s-MWCNTs (c) and (d), and 20/20/60 CuO/ZnO/p-MWCNTs (e) and (f)

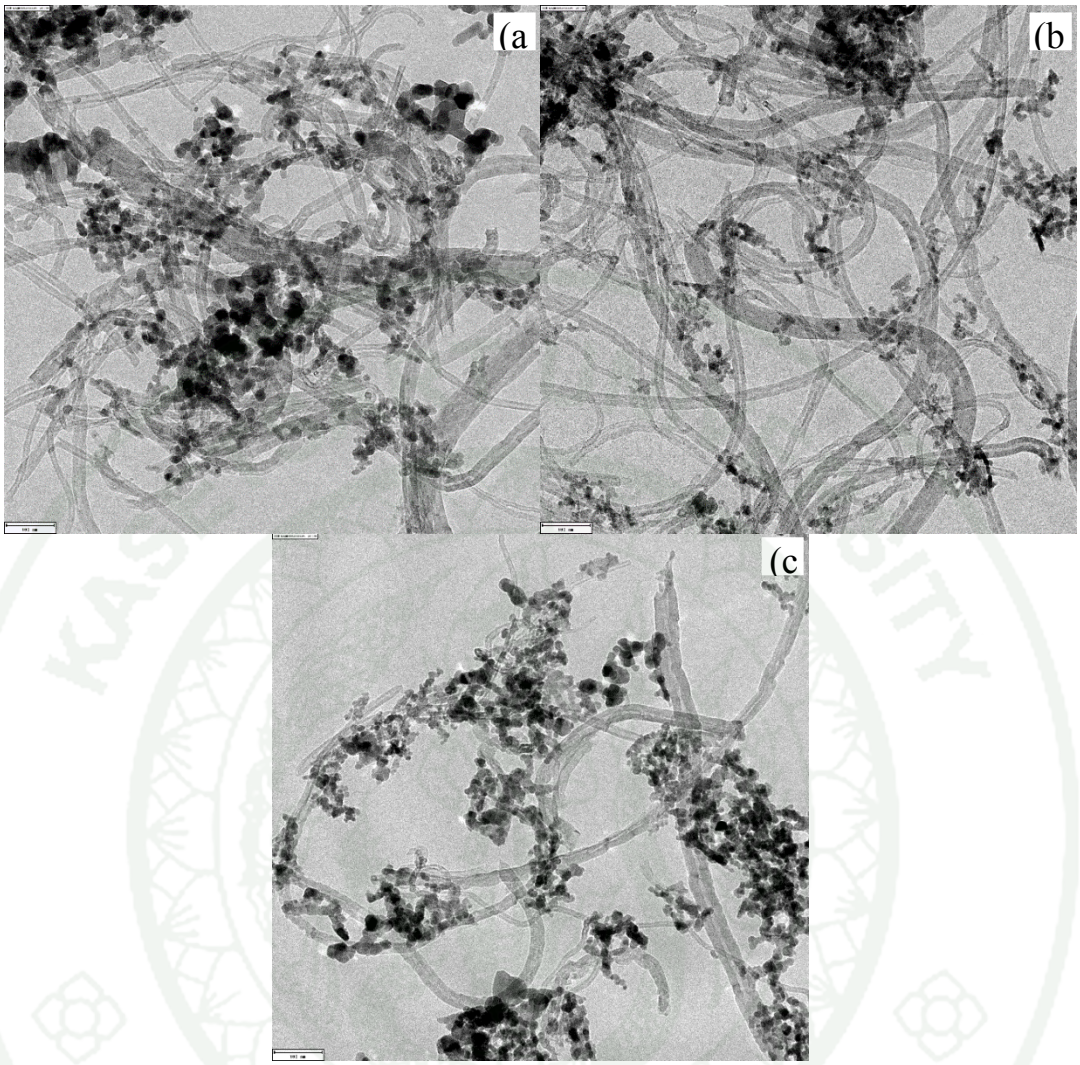

Figure 27 Transmission electron microscope images of 20/20/60 CuO/ZnO/MWCNTs (a), 20/20/60 CuO/ZnO/s-MWCNTs (b), and 20/20/60 CuO/ZnO/p-MWCNTs (c)

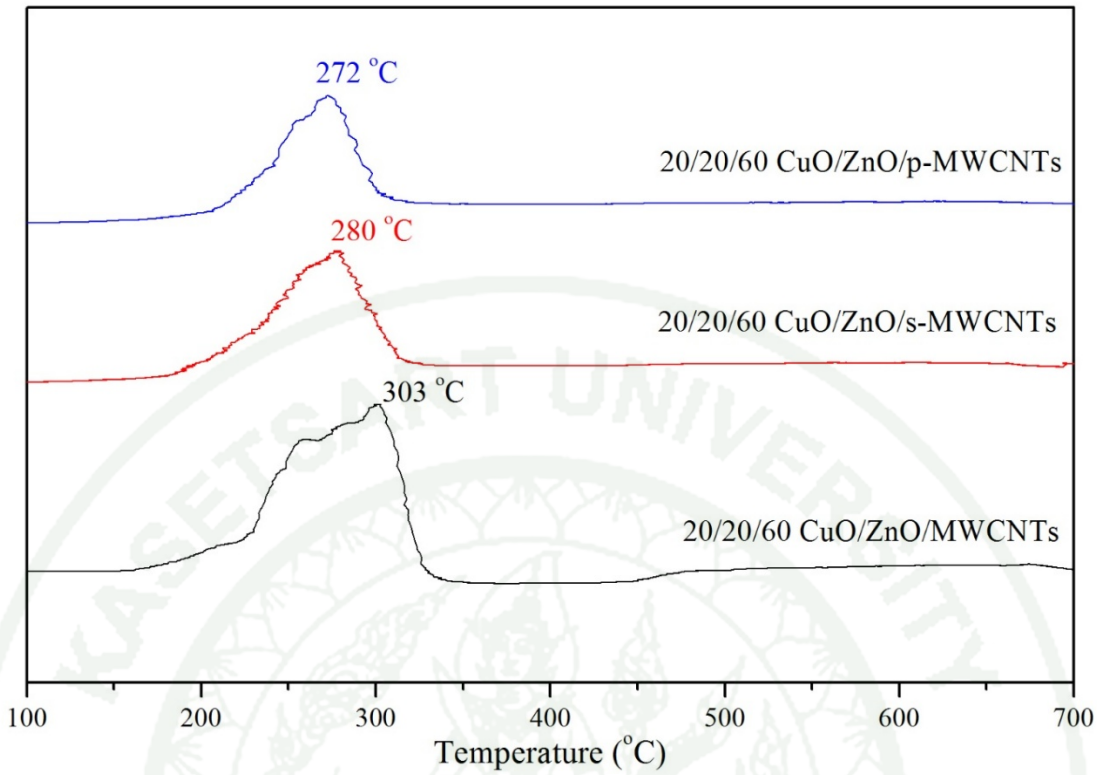

Figure 28 The reducibility of the catalysts

Figure 29 illustrated the XRD patterns of the pristine and functionalized MWCNTs catalysts. The XRD patterns of all catalysts exhibited peaks of similar pattern of CuO and ZnO. The monoclinic phase of copper oxide (CuO) was observed at 2θ of 35.5º, 38.7º, 48.7º, 61.5º, and 66.2º corresponding to the crystal planes of (-1 1 1), (1 1 1), (-2 0 2), (2 0 2), (-1 1 3) and (-3 1 1), respectively. The zinc oxide (ZnO) in hexagonal phase was observed at 31.8º, 34.5º, 36.3º, 47.7º, 56.7º, 63.0º, and 68.1º following the (1 0 0), (0 0 2), (1 0 1), (1 0 2), (1 1 0), (1 0 3), and (1 1 2) crystal planes, respectively. The peak of MWCNTs appeared at 26º and 43º which was correspondent with the crystal planes (0 0 2). Table 14 showed the CuO and ZnO crystal sizes of the catalysts that calculated at 38.4º and 31.8º. The catalysts with functionalized MWCNTs exhibited smaller crystallite size of the CuO and ZnO than the pristine one.

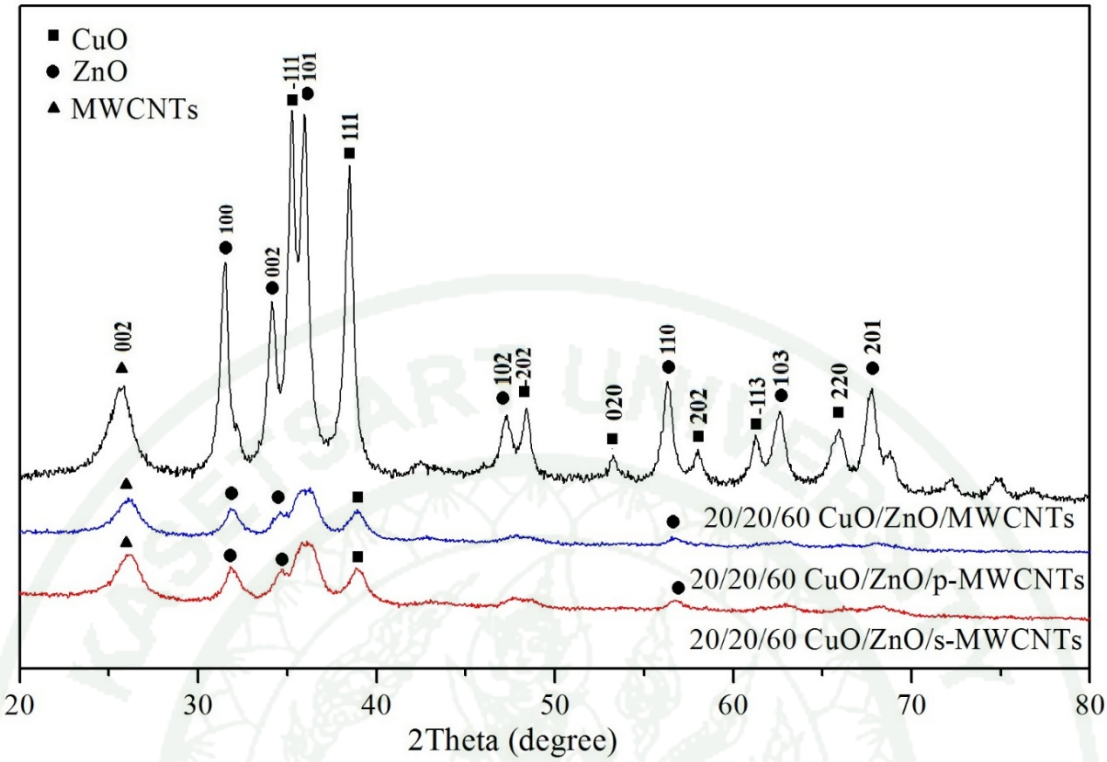

Figure 29 The XRD patterns of the catalysts

Table 14 The CuO and ZnO crystal sizes of catalysts

Catalyst	CuO crystal size (nm)	ZnO crystal size (nm)
20/20/60 CuO/ZnO/MWCNTs	19.12	18.70
20/20/60 CuO/ZnO/s-MWCNTs	9.88	9.99
20/20/60 CuO/ZnO/p-MWCNTs	10.34	10.57

3.2 Catalytic performance of CuO/ZnO/MWCNTs catalysts

The CO_2 conversion and methanol selectivity of the pristine and functionalized MWCNTs contents catalysts showed in Figure 30 and 31, respectively. The CO_2 conversion increased with the increasing reaction temperature. The highest CO_2 conversions exhibited on the sulfuric acid functionalized MWCNTs catalyst at 220 and 280 ºC were about 10 and 23 percent. But at 250 ºC, the highest CO_2

conversion shown on the phosphoric acid functionalized MWCNTs catalyst was about 18 percent and the sulfuric acid functionalized MWCNTs catalyst was 17 percent.Conversely, the methanol selectivity decreased increasing of reaction temperature. The highest percent of methanol selectivity obtained from the phosphoric acid functionalized MWCNTs catalyst at 220 and 280 ºC were 55 and 16 percent. But at 250 ºC, the highest methanol selectivity as shown on the sulfuric acid solution functionalized MWCNTs catalyst was 22 percent and 25 percent on the phosphoric acid solution functionalized MWCNTs catalyst. As shown in Figure 32, the CO selectivity increased with the reaction temperature rising and the lowest CO selectivity achieved on the phosphoric acid functionalized MWCNTs catalyst at 220 ºC was 45 percent. The methanol yield of the pristine and functionalized MWCNTs catalysts are shown in Figure 33, the highest methanol yield obtained from the sulfuric acid functionalized MWCNTs catalyst raised with the reaction temperature increasing from 220 ºC to the 250 ºC to be about 101 and 104 g/(kg cat. h) and then it was dropped to be 92 $g_{methanol}/(kg_{catalyst}$ h) at 280 ºC.

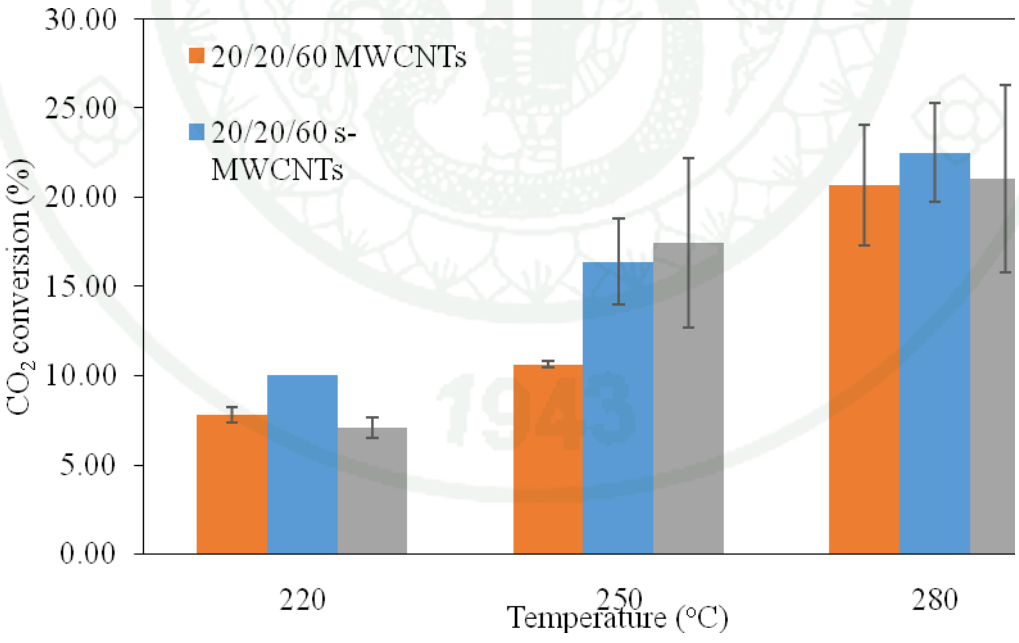

Figure 30 The CO_2 conversion of the catalysts

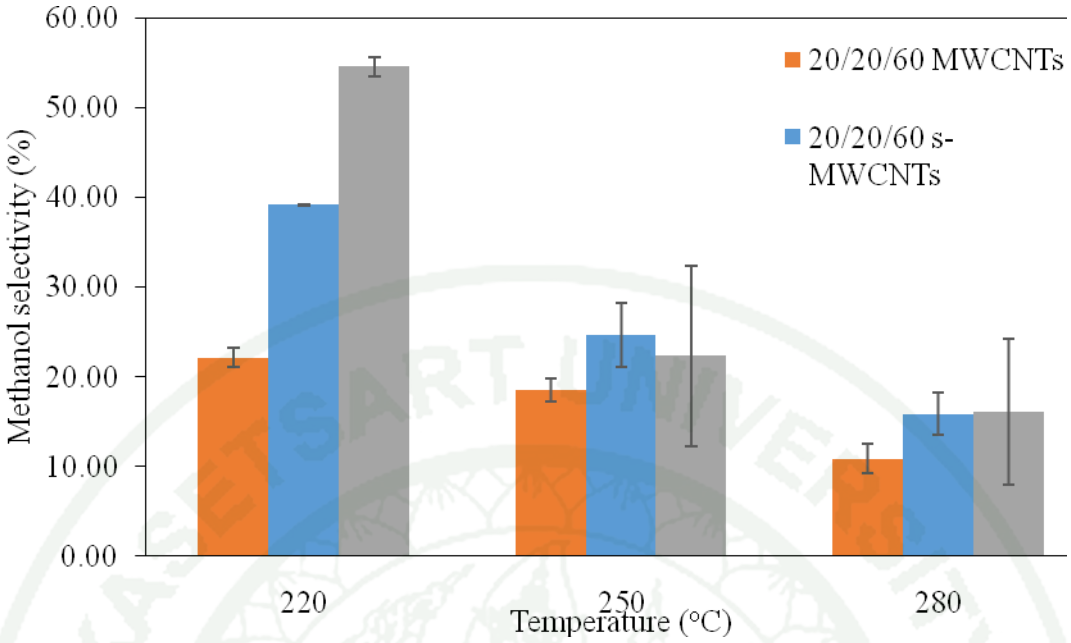

Figure 31 The methanol selectivity of the catalysts

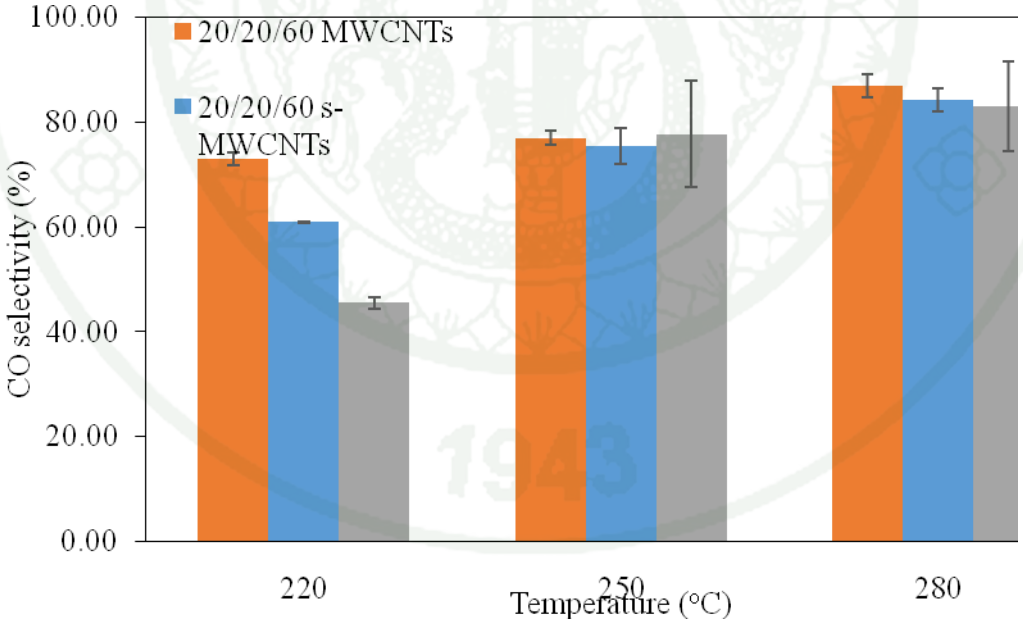

Figure 32 The CO selectivity of the catalysts

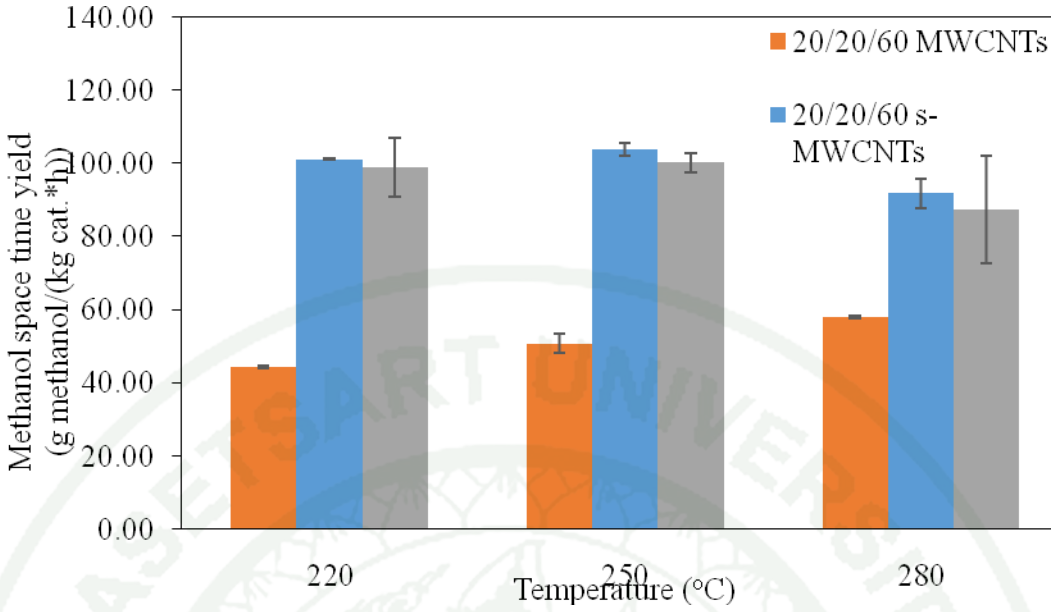

Figure 33 The methanol yield of the catalysts

CONCLUSION AND RECOMMENDATIONS

Conclusion

The synthesis of methanol via CO_2 hydrogenation over CuO/ZnO/MWCNTs catalysts was studied. Sulfuric and phosphoric acid solution showed high defection on the wall of carbon nanotubes and the 20/20/60 CuO/ZnO/MWCNTs ratio resulted in high methanol yield. Therefore, the 20/20/60 CuO/ZnO/MWCNTs was selected to prepare the 20/20/60 CuO/ZnO with functionalized carbon nanotubes. This catalyst with functionalized carbon nanotubes showed high performance for methanol synthesis presumably due to promoting hydrogen spillover on CNTs and better distribution of metallic particles. The CO_2 conversion and the methanol yield of catalysts increased with increasing reaction temperature. Despite lower CO_2 conversion, the methanol yield over 10/10/20 and 20/20/60 CuO/ZnO/MWCNT catalysts were remarkably higher than that of the CuO/ZnO catalyst. The improvement of methanol selectivity over the MWCNT and functionalized MWCNT added to CuO/ZnO would be describable to the better dispersion of metallic particles and hydrogen adsorbability of CuO/ZnO with functionalized carbon nanotubes.

Recommendations

Reducing CO_2 contents in our atmosphere is world-wide accepted to be one major solution for the green-house effect that ignited global warming.At its optimum achievement, the present study successed in synthesis of methanol from CO_2 by the selected catalysts. However, for more completion of any further studies of this most important issue, followings are recommendations to be noted.

1. The studies on better preparation methods for improving catalyst activity should be emphasized.

2. The CuO/ZnO with functionalized carbon nanotubes should be studied for synthesis of other hydrocarbon products as dimethyl ether.

LITERATURE CITED

Alpers, C.N., D.L. Dettman, K.C. Lohmann and D. Brabec. 1990. Stable Isotopes of Carbon Dioxide in Soil Gas over Massive Sulfide Mineralization at Crandon, Wisconsin **Journal of Geochemical Exploration** 38 (1-2): 69-86.

An, X., Y.Z. Zuo, Q. Zhang, D.Z. Wang and J.F. Wang. 2008. Dimethyl Ether Synthesis from CO_2 Hydrogenation on a CuO-ZnO-Al_2O_3-ZrO_2/HZSM-5 Bifunctional Catalyst. **Ind. Eng. Chem. Res.** 47: 6547-6554.

Baltes, C., S. Vukojevic and F. Schuth. 2008. Correlations Between Synthesis, Precursor, and Catalyst Structure and Activity of a Large Set of CuO/ZnO/Al_2O_3 Catalysts for Methanol Synthesis. **Journal of Catalyst** 258: 334-344.

Bhar, R. and A.G. Malliaris. 2011. Oil Prices and The Impact of The Financial Crisis of 2007–2009. **Energy Economics** 33 (6): 1049-1054.

Behrens M., I. Kasatkin, S. Kuhl, S. Zander, F. Girgsdies and R. Schlogl. 2012. The Active Site of Methanol Synthesis over Cu/ZnO/Al2O3 Industrial Catalyst, **Science** 336: 893-897.

Canadell, J.G., C. Le Quere, M.R. Raupach, C.B. Field, E.T. Buitenhuis and P. Ciais. 2007. Contributions to Accelerating Atmospheric CO2 Growth from Economic Activity, Carbon Intensity, and Efficiency of Natural Sinks. **Proc Natl Acad Sci U S A** 104 (47): 18866-18870.

Collins, S.E., J.J. Delgado, C. Mira, J.J. Calvino, S. Bernal and D.L. Chiavassa. 2012. The Role of Pd–Ga Bimetallic Particles in The Bifunctional Mechanism of Selective Methanol Synthesis via CO2 Hydrogenation on a Pd/Ga2O3 Catalyst. **Journal of Catalysis** 292: 90-98.

Dong, X., H.B. Zhang, G.D. Lin, Y.Z. Yuan and K.R. Tsai. 2003. Highly Active CNT-Promoted Cu-ZnO-Al_2O_3Catalyst for Methanol Synthesis from $H_2/CO/CO_2$. **Catalysis Letters** 85: 237-246.

Ereña, J., R. Garoña, J.M. Arandes, A.T. Aguayo and J. Bilbao. 2005. Effect of Operating Conditions on The Synthesis of Dimethyl Ether over a CuO-ZnO-Al2O3/NaHZSM-5 Bifunctional Catalyst. **Catalysis Today** 107-108: 467-473.

Friedrichs, J. 2010. Global Energy Crunch: How different parts of the world would react to a peak oil scenario. **Energy Policy** 38 (8): 4562-4569.

Fujitani, T., J. Nakamura. 1998. The Effect of ZnO in Methanol Synthesis Catalysts on Cu Dispersion and The Specific Activity. **Catalysis Letters** 56: 119-124.

Galvita, V.V.,G.L. Semin, V.D. Belyaev, T.M.Yurieva and V.A.Sobyanin. 2001. Production of Hydrogen from Dimethyl Ether. **Applied Catalysis A** 216: 85-90.

Guo, X.J., L.M. Li, S.M. Lui, G.L. Bao and W.H. Hou. 2007. Preparation of CuO/ZnO/Al_2O_3 Catalysts for Methanol Synthesis Using Parallel-Slurry-Mixing Method. **Journal of Fuel Chemistry and Technology** 35(3): 329-333.

Guo, X.M., D.S. Mao, S. Wang, G.S. Wu and G.S. Lu. 2009. Combustion Synthesis of CuO-ZnO-ZrO_2 Catalysts for the Hydrogenation of Carbon Dioxide to Methanol. **Catalysis Communications** 10: 1661-1664.

Her, S.C. and C.Y. Lai. 2013. Dynamic Behavior of Nanocomposites Reinforced with Multi-walled Carbon Nanotubes (MWCNTs). **Materials** 6: 2274-2284.

Hodkiewicz, J. 2010. Characterizing Carbon Materials with Raman Spectroscopy. **Thermo Fisher Scientific** 3:1112-1115.

Hooijdonk, E.V., C. Bittencourt, R. Snyders and J.F. Colomer. 2013. Functionzalization of Vertically Aligned Carbon Nanotubes. **Beilstein Jpurnal of Nanotechnology** 4:129-152.

Jun, K.W., W.J. Shen, K.S. Rama Rao and K.W. Lee. 1998. Residual Sodium Effect on the Catalytic Acitivity of $Cu/ZnO/Al_2O_3$ in Methanol Synthesis from CO_2 hydrogrnation. **Applied Catalyst A: General** 174: 231-238.

Kim, M.S., Lee, H.S., Yoo, S.J., Youn, Y.S. and Lee, Y.W., 2013, Simultaneous Synthesis of Biodiesel and Zinc Oxide Nanoparticles Using Supercritical Methanol. **Fuel** (109): 279-284.

Ko, J.H., Kang, K.M., Park, S.H. and Kim, W.G., 2014. Effect of Design of Multilayer Electrodes in Direct Methanol Fuel Cells (DMFCs). **International Journal of Hydrogen Energy** (39): 1571-1579.

Liu, P., Y. Yang and M.G. White. 2013. Theoretical Perspective of Alcohol Decomposition and Synthesis from CO2 Hydrogenation. **Surface Science Reports** 68 (2): 233-272.

Ma, P.C., N.A. Siddiqui, G. Marom and J.K. Kim. 2010. Dispersion and Functionalization of Carbon Nanotubes for Polymer-Based Composites: A review. **Composites: Part A** 41: 1345-1367.

Mahittikul, A., P. Prasassarakich and L.R. Garry, 2009, Hydrogenation of Natural Rubber Latex in The Presence of $[Ir(cod)(PCy_3)(py)]PF_6$. **Journal of Molecule Catalyst A** 297: 135-141.

Mistry, S.R. and K.C. Maheria. 2012. Synthesis of Diarylpyrimidinones (DAPMs) Using Large Pore Zeolites. **Journal of Molecular Catalysis A: Chemical** 355: 210-215.

Naseh, M.V., A.A. Khodadadi, Y. Mortazari, A. Sahraei, F. Pourfayaz and S.M. Sedghi. 2009. Functionalization of Carbon Nanotubes Using Nitric Acid Oxidation and DBD Plasma. **International Journal of Chemical and Biological Engineering** 2(2): 66-68.

Osswald, S., M. Havel and Y. Gogotsi. 2007. Monitoring Oxidation of Multiwalled Carbon Nanotubes by Raman Spectroscopy. **Journal of Raman Spectroscopy** 38; 728-736.

Rafferty, J.L., J.I Siepmann,. and M.R. Schure, 2011. Mobile Phase Effects in Reversed-Phase Liquid Chromatography: A Comparison of Acetonitrile/Water and Methanol/Water Solvents as Studied by Molecular Simulation. **Journal of Chromatography A** (1218): 2203-2213.

Rhodes, M.D. and A.T. Bell, 2005. The Effects of Zirconia morphology on Morphology on Mehtanol Synthesis from CO and H2 over Cu/ZrO2 Catalysts Part I. Steady-state studies. **Journal of Catalysis** 233: 198-209.

Rodriguez-Reinoso, F. 1998. The Role of Carbon Materials in Heterogeneous Catalyst. **Carbon** 36: 159-175.

Shao, D.D., G.D. Sheng, C.G. Chen, X.K. Wang and M. Nagatsu. 2010. Removal of Polychlorinated Biphenyls from Aqueous Solutions Using β-Cyclodextrin Grafted Multiwalled Carbon Nanotubes. **Chemosphere** 79: 679-685.

Shin, E. 1982. The Impact of The First Oil Crisis On Energy Demand in Korea. **Energy Economics**4 (4):259-267.

Shina, H.Y., Ryua, J.H., Baea, S.Y. and Kim, Y.C., 2013. Biodiesel Production from Highly Unsaturated Feedstock via Simultaneous Transesterification and Partial Hydrogenation in Supercritical Methanol. **Journal Of Supercritical Fluids** (82): 251-255.

Sun, Q., Y.L. Zhang, H.Y. Chen, J.F. Deng, D. Wu and S.Y. Chen, 1997. A Novel Process or the Preparation of Cu/ZnO and Cu/ZnO/Al_2O_3 Ultrafine Catalyst: Structure, Sureface Properties, and Activity for Methanol Synthesis from CO_2+H_2. **Journal of Catalysis** 167: 92-105.

Suzuki, K. 2009. Quantitative Measurements of Brønsted Acidity in Zeolites by Ammonia IRMS-TPD Method. **Graduate School of Engineering, Tottori University**: 2.

Wikipedia The Free Encyclopedia. 2013. **Dimethyl Ether**. Available Source: http://en.wikipedia.org/wiki/Dimethyl_ether. September, 2013.

Witoon, T., T. Permsirivanich, W. Donphai, A. Jaree and M. Chareonpanich. 2013. CO_2 Hydrogenation to Methanol over Cu/ZnO Nanocatalysts Prepared via a Chitosan-Assisted Co-precipitation Method. **Fuel Processing Technology** 116: 72-78.

Xin, A., Z. Yizan, Z. Qiang and W. Jinfu. 2009. Methanol Synthesis from CO2 Hydrogenation with a Cu/Zn/Al/Zr Fibrous Catalyst. **Chinese Journal of Chemical Engineering** 17 (1): 88-94.

Yang, Y., S.Q. Qui, C.G. He, W.J. He, L.J. Yu and X.L. Xie. 2010. Green Chemical Functionalization of Multiwalled Carbon Nanotubes with Poly(ε-caprolactone) in ionic Liquids. **Applied Surface Science** 257: 1010-1014.

Yudianti, R., H. Onggo, Sudirman, Y. Saito, T. Iwata and J.-I. Azuma. 2011. Analysis of Functional Group Sited on Multi-Wall Carbon Nanotube Surface. **The Open Materials Science Journal** 5: 242-247.

Zhang, H., X. Dong, G.D. Lin, Y.Z. Yuan and K.R. Tsai. Methanol Synthesis from H_2/CO/CO_2 over CNTs-Promoted Cu-ZnO-Al_2O_3 Catalyst. **Fuel Chemistry Division Preprints** 47(1), 284-285.

Zhang, Q., Y.Z. Zuo, M.H. Han, J.F. Wang, Y. Jin and F. Wei. 2010. Long Carbon Nanotubes Intercrossed Cu/Zn/Al/Zr Catalyst for CO/CO2 Hydrogenation to Methanol/Dimethyl Ether. **Catalyst Today** 15: 55-60.

Zahedi, G., A. Elkamel and A. Lohi. 2007. Enhancing CO_2 Conversion to Methanol Using Dynamic Optimization, Applied on Shell Temperature and Intel Hydrogen During Four Years Operation of Methanol Plant, **Energy Source Part A**. 29: 1385-1396.

APPENDIX

CALCULATIONS

1. Metal surface area

$$A = S_f \times \frac{V_{ads}}{V_g} \times \frac{100\%}{\%M} \times N_A \times \sigma_m \times \frac{m^2}{10^{18}\, nm^2}$$

where

S_f = the chemisorptions stoichiometry (=2)

V_{ads} = the volume of chemisorbed gas required to form the monolayer (cm^3/g)

V_g = the volume of gas at STP (= 22,414 cm^3/mol)

$\%M$ = the metal loading percentage

N_A = the Avogado's number (= 6.02×10^{23} mol^{-1})

σ_m = the surface area occupied by one atom (= 0.06849 nm)

2. Dispersion

$$\%D = S_f \times \frac{V_{ads}}{V_g} \times \frac{MW}{\%M} \times 100\% \times 100\%$$

where

S_f = the chemisorptions stoichiometry (=2)

V_{ads} = the volume of chemisorbed gas required to form the monolayer (cm^3/g)

V_g = the volume of gas at STP (= 22,414 cm^3/mol)

$\%M$ = the metal loading percentage

MW = the molecular weight of metal (= 63.546 g/mol)

3. Average metal particle size

$$d = \frac{f}{\rho_m \times A} \times \frac{m}{10^6\ cm^3}$$

where

f = the shape factor (constant = 6)

ρ_m = the density of metal (= 8.92 g/cm^3)

A = the specific metal surface area

4. Metal crystallite size (Scherrer's equation)

$$\tau = \frac{K\lambda}{\beta \cos\theta}$$

where

τ = the mean size of the crystalline (nm)

K = the dimensionless shape factor

λ = the X-ray wavelength (nm)

β = the line broadening at half the maximum intensity

θ = the Bragg angle

CURRICULUM VITAE

NAME : Ms. Pussorn Akkarapreechakul

BIRTH DATE : Novenber, 1989

BIRTH PLACE : Chachoengsao, Thailand

EDUCATION :

YEAR	**INSTITUTE**	**DEGREE/DIPLOMA**
2011	Kasetsart University	B. Eng (Chemical Engineering)

POSITION/TITLE : -

WORK PLACE : -

SCHOLARSHIP/AWARDS: TAIST Tokyo Tech (Thailand Advanced Institute of Science and Technology) Program at the faculty of Engineering, Kasetsart Universityunder the National Science and Technology Development Agency 2012-2014

INTERNATIONAL PUBLICATIONS

1) Akkarapreechakul, P., T.Witoon, K. Faungnawakij and W. Tanthapanichakoon. Cu DECORATING OF FUNCTIONALIZED MULTI-WALLED CARBON NANOTUBES. 2014. Pure and Applied Chemistry International Conference 2014 (PACCON2014). 530-533.

2) Akkarapreechakul, P., T.Witoon, K. Faungnawakij and W. Tanthapanichakoon. Methanol Synthesis via CO2Hydrogenation over CuO/ZnO/CNTs Catalysts.2014. 3rdInternational Conference on Environmental Engineering, Scienceand Management.